AN ABSTRACT OF THE THESIS OF

ROBERT FOISY ADRION for the M.S. in Electrical Engineering
(Name) (Degree) (Major)

Date thesis is presented 18 August 1965

Title SPHERICAL MIRROR RESONATORS AND OPTICAL MODE SELECTION

Abstract approved [redacted]
(Major professor)

This is a review paper based on recent literature in the areas of spherical mirror resonators and optical mode selection. The Fabry-Perot interferometer with spherical mirrors has been widely used as a laser resonator. The modes of oscillation, diffraction losses and resonance condition are determined for the confocal resonator, i.e. a resonator with mirror spacing equal to the common radius of curvature of the mirrors. Resonators with nonconfocal spacing and mirrors of different curvature are described in terms of an equivalent confocal resonator. It is shown that any spherical mirror resonator may be characterized as high loss or low loss according to the geometry of the resonator.

Lasers using spherical mirror resonators will oscillate in several modes simultaneously, because of the interaction of the broad emission line of the laser active medium and the closely spaced

mode resonances. For many applications a single frequency output is desirable, and methods must be employed to suppress unwanted oscillations. Unwanted modes may be suppressed by placing absorbing materials within the resonator and by adding devices to the resonator which act as bandpass filters.

SPHERICAL MIRROR RESONATORS AND OPTICAL MODE SELECTION

by

ROBERT FOISY ADRION

A THESIS

submitted to

OREGON STATE UNIVERSITY

in partial fulfillment of
the requirements for the
degree of

MASTER OF SCIENCE

June 1966

APPROVED:

[redacted]

Associate Professor of Electrical Engineering

In Charge of Major

[redacted]

Head of Department of Electrical Engineering

[redacted]

Dean of Graduate School

Date thesis is presented 18 August 1965

Typed by Nancy Kerley

TABLE OF CONTENTS

TABLE OF CONTENTS (continued)

LIST OF FIGURES

LIST OF FIGURES (continued)

SPHERICAL MIRROR RESONATORS AND OPTICAL MODE SELECTION

INTRODUCTION

The Fabry-Perot interferometer (4) has found widespread use as a laser optical resonator. This type of interferometer consists of two reflecting plates, or mirrors, aligned along a central axis which is normal to the reflecting surfaces. For laser applications, the reflecting surface is usually either plane or spherical. The first lasers used plane mirror resonators. However, it was found that the alignment of the plane mirrors was very critical, especially in the long resonators used for gas lasers. For example, one gas laser would not operate if its mirrors were out of parallelism by more than one second of arc (19). Such a small alignment tolerance is undesirable, because the proper operation of the laser would depend critically on mechanical and thermal fluctuations in the laser's surroundings. These fluctuations could cause misalignment of the plane mirrors. Also, departure from perfect flatness could cause alignment problems. The alignment tolerance of the spherical mirror resonator is much larger than that of the plane mirror resonator. In one instance (31) the spherical mirrors of a gas laser were misaligned by 13 minutes of arc and the laser kept operating, although with power output reduced by one-half. It is because of this much greater alignment

tolerance that the spherical mirror resonator has been more widely used as a laser resonator than the plane mirror resonator.

When a spherical mirror resonator is used as the resonant cavity of a laser, an active medium fills part or all of the volume between the mirrors. If an arbitrary electromagnetic wave leaves one mirror, it will be amplified by the active medium as it travels toward the second mirror. However, the wave will be attenuated by scattering losses introduced by medium inhomogeneties (2). When the wave arrives at the second mirror, it will be further attenuated by mirror losses resulting from imperfect reflection at the mirror. Also, the diffractive spread of the wave will cause a loss at the second mirror because of a diffractive spillover of energy around the mirror edges (12). If the wave gains enough energy as it passes through the active medium to compensate for these losses, oscillation may occur.

The ratio of power losses per unit cross-sectional area caused by scattering to the incident power, i.e. the percent scattering losses, depends only on the homogeneity of the medium, and the percent reflection losses depend only on the mirror properties. However, the diffraction losses are dependent on the distribution of the fields within the resonator (2). Therefore, the diffraction losses determine the field distribution within the resonator during oscillation in the following manner. The field distribution of an arbitrary

wave leaving one mirror will be changed by diffraction losses as it bounces back and forth between the mirrors, until a self-reproducing distribution will be set up; i.e. a wave with a certain field distribution at one mirror will have the same distribution (within a constant) after one round trip in the resonator. This type of traveling wave is present when standing waves occur in the resonator. The field configuration within the resonator associated with such a self-reproducing wave is a normal mode of oscillation of the resonator. A normal mode is independent of the initial wave and depends only on the resonator geometry and medium. Assuming that the propagation characteristics of the resonator medium are essentially those of a uniform dielectric (i.e. that the resonator medium is linear, isotropic, homogeneous, and non-dissipative) we should be able to find these normal modes by investigating a passive resonator which is immersed in a uniform dielectric. The normal modes found for this passive resonator will be very nearly the modes of oscillation of a gas laser, because the propagation characteristics of the low-density gaseous medium are approximately those of a uniform dielectric. A typical solid state laser material, however, is not well described as a uniform dielectric in the neighborhood of the frequency of interest because of the high density of active particles. Therefore the passive resonator modes may not accurately represent the solid state laser fields; however, they should describe at least the gross features

of the fields in the solid state laser. Note that the finite lateral extent of the active medium of both solid state and gas lasers will introduce additional perturbation to the passive resonator modes.

Let us see how the normal modes of a passive resonator can be found. Consider a passive resonator having perfectly reflecting mirrors. Mirror loss caused by imperfect reflection will not seriously affect the normal mode field distributions as long as the losses are small and fairly uniform over the mirrors (5). Suppose we introduce optical energy into the resonator in the form of an arbitrary wave traveling from one mirror toward the other. After a transient period the field distribution in the resonator will be that of one (or a sum) of the resonator's normal modes of oscillation. The amplitude of the normal mode will then decay with time because of diffraction losses. Analogous to this is the damped-sinusoid response of an underdamped parallel RLC circuit with an initial DC voltage on the capacitor.

The normal modes of a spherical mirror resonator may be found by applying the Huygens-Fresnel principle, which is derived in Appendix 1. This principle states that if a point P is in a linear, isotropic, homogeneous, source-free medium which is enclosed by a closed surface s; and if point P and surface s are located in the far zone of all sources; and if point P is located such that the distance r from P to an arbitrary point on s is much greater than a wave length,

then the field at point P is

$$u_p = \frac{-ik}{2\pi} \int_s u \cos(\bar{n}, \bar{r}) \frac{e^{-ikr}}{r} ds \qquad (1-1)$$

where u_p and u represent any one of the rectangular components of the electromagnetic field at point P and surface s respectively, $\bar{n}$ is an inward normal of the surface s, and $k = \omega\sqrt{\mu\epsilon}$ is the propagation constant of the medium in which P is located.

Consider Figure 1. M_1 and M_2 represent the two mirrors of an optical resonator. The screen is far from the sources which produced the incident field. The opening in the screen coincides with mirror one; surface A is a portion of the backside of the screen; and surface B is a large sphere of radius R centered at P. The surfaces M_1, A, and B form a closed surface which encloses P. We can find the field at P by applying the Huygens-Fresnel principle, assuming that the conditions governing its application are satisfield. Therefore,

$$u_p = \frac{-ik}{2\pi} \int_{M_1+A+B} u \cos(\bar{n}, \bar{r}) \frac{e^{-ikr}}{r} ds \qquad (1-2)$$

We can set u = 0 on A, because A is shielded from the incident field by the screen. Assume that the sphere B is made of some perfectly absorbing substance. Then the contribution to the field at P from the surface B is zero. Therefore the field at P is

$$u_p = \frac{-ik}{2\pi} \int_{M_1} u \cos(\bar{n}, \bar{r}) \frac{e^{-ikr}}{r} \, ds \qquad (1\text{-}3)$$

This technique will allow us to find the normal mode fields of the resonator.

Solution for the normal modes leads to the determination of the diffraction losses associated with each mode and the resonance conditions of spherical mirror resonators. The normal modes are characterized by longitudinal and transverse periodicity, and the frequency of oscillation is determined by the number of longitudinal and transverse variations in the normal mode field configuration. Because the emission lines of laser materials are generally broader than the frequency separation between adjacent mode resonances, a laser using a spherical mirror resonator will oscillate in several different normal modes simultaneously.

It is often desirable to limit the number of modes in which a laser oscillates. This limitation is imposed by selective attenuation of the undesired modes. Mode selection with respect to transverse field variations is accomplished by purposely enhancing diffraction losses or by inserting an absorbing material within the resonator. Longitudinal mode selection involves the addition to the resonator of devices which act as bandpass filters. Single frequency optical output from mode selective gas lasers has been observed (15; 21).

This is a review paper which is based on recent literature

in the areas of spherical mirror resonators and optical mode selection.

THE CONFOCAL RESONATOR

Formulation of the Problem

Consider a resonator consisting of two identical, perfectly reflecting spherical mirrors with radius of curvature b, which are placed so that the distance d between the mirrors is equal to b (see Figure 2). Since the focal length of a spherical mirror is one-half of its radius of curvature, the foci of the two mirrors coincide, and therefore the resonator is called a confocal resonator. Assume that all resonator dimensions are $\gg \lambda$. The mirrors are assumed to have a square cross section with dimensions 2a by 2a, and a is much less than the spacing b.

Suppose an initial wave is launched from mirror 1 (M_1) toward mirror 2 (M_2). Assume that the field is linearly polarized in the y direction (5). If the initial wave has an electric field distribution $E(x_1, y_1)$, then the electric field of the wave incident on M_2 is

$$E'(x', y') = \frac{ik}{2\pi} \int_{M_1} E(x_1, y_1) \frac{e^{-ikR}}{R} \, dx_1 dy_1 \qquad (2\text{-}1)$$

Since $\cos(\bar{n}, \bar{r}) \cong -1$ when $a \ll b$. Now this wave is reflected from M_2 back toward M_1, and then it is reflected from M_1 with some field distribution $E''(x, y) = \frac{ik}{2\pi} \int_{M_2} E'(x', y') \frac{e^{-ikR'}}{R'} \, dx' dy' \qquad (2\text{-}2)$

If normal modes of oscillation exist, then $E''(x, y)$ must be equal to

$E(x, y)$ within a constant multiplier, so set

$$E''(x, y) = \sigma^2 E(x, y) \tag{2-3}$$

Combining equations (2-1), (2-2), and (2-3), we can write

$$\sigma^2 E(x, y) = \frac{-k^2}{4\pi^2} \int_{M_2} \int_{M_1} E(x_1, y_1) \frac{e^{-ikR}}{R} \, dx_1 dy_1 \frac{e^{-ikR'}}{R'} \, dx' dy' \tag{2-4}$$

Since R' is not a function of x_1 or y_1, the order of integration in equation (2-4) can be changed and it can be written (7) as

$$\sigma^2 E(x, y) = \frac{-k^2}{4\pi^2} \int_{M_1} K(x, x_1; y, y_1) E(x_1, y_1) \, dx_1 dy_1 \tag{2-5}$$

where the kernel

$$K(x, x_1; y, y_1) = \int_{M_2} \frac{e^{-ik(R+R')}}{RR'} \, dx' dy' \tag{2-6}$$

Having obtained equation (2-5), we can now find the normal mode field distributions over the mirrors. The field distributions to which we refer are those of either the incident or reflected normal mode traveling waves, not the sum of the two waves. This sum is zero over the surface of the perfectly reflecting mirrors.

Normal Mode Solutions

Eigenfunctions

For the resonator shown schematically in Figure 2, it has been shown (36) that, for $x, y \ll b$,

$$R \cong d - \frac{x_1x' + y_1y'}{d} - \frac{d-b}{2bd}\,(x_1^2 + x'^2 + y_1^2 + y'^2)$$

and (2-7)

$$R' \cong d - \frac{xx' + yy'}{d} - \frac{d-b}{2bd}\,(x^2 + x'^2 + y^2 + y'^2)$$

For the confocal case considered here, d = b, and equations (2-7) become

$$R \cong b - \frac{x_1x' + y_1y'}{b}$$

$$R' \cong b - \frac{xx' + yy'}{b} \qquad (2-8)$$

Now for x, y $\ll$ b we can let RR' = b^2 in equation (2-6), but in the exponential term equations (2-8) should be used. Then equation (2-6) becomes

$$K(x, x_1; y, y_1) = \frac{e^{-i2kb}}{b^2} \int_{-a}^{a} e^{i\frac{k}{b}x'(x+x_1)}\,dx' \int_{-a}^{a} e^{i\frac{k}{b}y'(y+y_1)}\,dy' \qquad (2-9)$$

When evaluated this yields

$$K(x, x_1; y, y_1) = \frac{4e^{-i2kb}}{k^2} \cdot \frac{\sin\frac{ka}{b}(x+x_1)}{(x+x_1)} \cdot \frac{\sin\frac{ka}{b}(y+y_1)}{(y+y_1)} \qquad (2-10)$$

Assume that (5) E(x, y) can be written as Eo fm(x)g_n(y), and let $\sigma^2 = \sigma_m^2\,\sigma_n^2$. Then equation (2-5) can be written as

$$\sigma_m^2\,\sigma_n^2\,f_m(x)\,g_n(y) = -e^{-i2kb} \int_{-a}^{a} f_m(x_1)\,\frac{\sin\frac{ka}{b}(x+x_1)}{\pi(x+x_1)}\,dx_1$$

$$\cdot \int_{-a}^{a} g_n(y_1)\,\frac{\sin\frac{ka}{b}(y+y_1)}{\pi\,(y+y_1)}\,dy_1 \qquad (2-11)$$

Equation (2-11) can be written as two homogeneous Fredholm integral equations of the second kind (7;26):

$$\sigma_m^2 f_m(x) = i e^{-ikb} \int_{-a}^{a} f_m(x_1) \frac{\sin \frac{ka}{b} (x+x_1)}{\pi (x+x_1)} dx_1 \qquad (2-12)$$

and

$$\sigma_n^2 g_n(y) = i e^{-ikb} \int_{-a}^{a} g_n(y_1) \frac{\sin \frac{ka}{b} (y+y_1)}{\pi(y+y_1)} dy_1 \qquad (2-13)$$

Now define the dimensionless variables (5) $c = \frac{a^2 k}{d} = 2\pi \frac{a^2}{b\lambda}$, $X = \frac{x\sqrt{c}}{a}$, $Y = \frac{y\sqrt{c}}{a}$, and let $F_m(X) = f_m(x)$, $G_n(Y) = g_n(y)$. Equations (2-12) and (2-13) have the same form, so consider (2-12). In terms of the new variables equation (2-12) becomes

$$\sigma_m^2 F_m(X) = i e^{-ikb} \int_{-\sqrt{c}}^{\sqrt{c}} F_m(X_1) \frac{\sin \frac{ka^2}{b} (X/\sqrt{c} + X_1/\sqrt{c})}{\pi(X/\sqrt{c} + X_1/\sqrt{c})} dX_1/\sqrt{c} \qquad (2-14)$$

The angular prolate spheroidal wave functions $S_{om}(c, t)$ satisfy this relation (6, 35):

$$\frac{2c}{\pi} [R_{om}^{(1)}(c, 1)]^2 S_{om}(c, t) = (-1)^m \int_{-1}^{1} S_{om}(c, s) \frac{\sin c(t+s)}{\pi(t+s)} ds \qquad (2-15)$$

$$m = 0, 1, 2, \ldots\ldots$$

where $R_{om}^{(1)}(c, 1)$ is the radial prolate spheroidal wave function. After comparing equations (2-14) and (2-15), it is evident that

$$F_m(X) \propto S_{om}(c, X/\sqrt{c}) = S_{om}(c, n_x) \qquad (2-16)$$

where $n_x = x/a$. Also we can see that

$$\sigma_m^2 = i\, e^{-ikb}\, (-1)^m\, \frac{2c}{\pi}\, [R_{om}^{(1)}(c,1)]^2 \qquad (2\text{-}17)$$

So, for a given value of c, there is an infinite number of characteristic solutions, or eigenfunctions, $S_{om}(c, n_x)$ of equation (2-14) and associated with each eigenfunction is its eigenvalue σ_m^2. The eigenfunctions of equations (2-11) are

$$f_m(x)\, g_n(y) \propto S_{om}(c, x/a)\, S_{on}(c, y/a) \qquad (2\text{-}18)$$

Notice that since the eigenfunctions are real, the mirrors are constant phase surfaces. The values of the spheroidal wave functions have been computed for various values of c (5). The parameter c may be written as $2\pi N$, where $N = \frac{a^2}{b\lambda}$. The parameter N is the Fresnel number and is so called because it is approximately equal to the number of Fresnel diffraction zones on one mirror as seen from the other mirror (12).

For $n_x^2 \ll 1$, (near the mirror center), and for large c, equation (2-16) can be written as (5)

$$F_m(X) \cong A_m\, H_m(X)\, e^{-X^2/2}$$

or

$$F_m(c, n_x) \cong A_m\, H_m(\sqrt{c}\, n_x)\, e^{-\frac{cn_x^2}{2}} \qquad (2\text{-}19)$$

where the $H_m(X)$ are the Hermite polynomials and A_m is an arbitrary normalizing constant. Similarly,

$$G_n(c, n_y) \cong A_n\, H_n(\sqrt{c}\, n_y)\, e^{-\frac{cn_y^2}{2}} \qquad (2\text{-}20)$$

where $n_y = y/a$. So the normal mode field distribution across mirror 1 is approximately a Gaussian times a Hermite polynomial. This eigenfunction approximation is exact only in the limit $c \to \infty$. Some of the eigenfunctions given by equation (2-19) are shown in Figure 3. The normalizing constant A_m is such that $F_m(0) = \pm 1$ for m even (5). Note that the field is concentrated near the mirror center for larger values of c, while the field becomes fairly large at the mirror edges for smaller values of c. So we should expect the diffraction losses to increase with decreasing c (or decreasing Fresnel number N).

So far we have found the field distributions across mirror 1 only. However, the symmetry of the resonator requires that the field distributions on mirror 2 be identical to those on mirror 1.

Resonance Condition

The eigenvalue $\sigma_m^2 \sigma_n^2$ of equation (2-11) can be written as

$$\sigma_m^2 \sigma_n^2 = -(-1)^m (-1)^n e^{-i2kb} \left(\frac{2c}{\pi}\right)^2 [R_{om}^{(1)}(c,1)]^2 [R_{om}^{(1)}(c,1)]^2 \qquad (2\text{-}21)$$

The phase angle of $\sigma_m^2 \sigma_n^2$ is the round trip phase shift from mirror 1 to mirror 2 and back to mirror 1. For resonance, the magnitude of the round trip phase shift must be equal to $2\pi q$, where $q = 1, 2, 3, \ldots\ldots$. This condition on the phase angle of $\sigma_m^2 \sigma_n^2$ is also implied by the fact that the eigenvalues of a homogeneous Fredholm

equation with a real symmetric kernel [equations (2-12) and (2-13)] are real (9). Now, since $(-1) = e^{i\pi}$, we can write

$$2\pi q = \left|(m+n+1)\pi - 2kb\right|$$

or

$$\frac{4b}{\lambda} = 2q + (m+n+1) \qquad (2\text{-}22)$$

$$q = 1, 2, \ldots; \; m, n = 0, 1, 2, \ldots$$

since $k = \frac{2\pi}{\lambda}$. Equation (2-22) is the resonance condition of the confocal resonator. Since the right side of equation (2-22) can take only integral values, then $\frac{4b}{\lambda}$ must be integral. There is much degeneracy in the frequency spectrum; e.g., increasing the sum (m+n) by two and decreasing q by one does not change the frequency. The frequency degenerate modes are orthogonal over the mirror surface; because the eigenfunctions corresponding to these modes satisfy the previously mentioned Fredholm equations and have different eigenvalues (5, 9). Since the curvature of the wavefront is small, the axial fields are negligible and the modes can be labeled as TEM_{mnq}, where $m, n = 0, 1, 2, \ldots$ refer to variations in the x and y directions, and q is the number of half wavelengths in the standing wave pattern between the mirror.

Diffraction Losses

We have shown that if a wave having field distribution

$E_o f_m(x)\, g_n(y)$ leaves mirror 1 and makes a round trip to mirror 2 and back to 1, the resulting wave leaves mirror 1 with a distribution $\sigma_m^2\, \sigma_n^2\, E_o\, f_m(x)\, g_n(y)$. Since the mirrors are identical, the same initial wave leaving mirror 1 arrives at mirror 2 with a field distribution $\sigma_m\, \sigma_n\, E_o\, f_m(x)\, g_n(y)$. If E(1) represents the electric field leaving mirror 1 and E(2) represents the electric field arriving at mirror 2, then

$$\frac{|E(2)|^2}{|E(1)|^2} = \frac{|\sigma_m \sigma_n E(1)|^2}{|E(1)|^2} = |\sigma_m \sigma_n|^2 \qquad (2\text{-}23)$$

The diffractive spread of the wave causes a diffraction loss at the second mirror. The time average energy storage per unit length (of z) of the wave leaving mirror 1 is approximately

$$W(1) = \frac{\epsilon}{2} \int_{-a}^{a} \int_{-a}^{a} |E(1)|^2 \, dx\, dy$$

Similarly the energy storage per unit length of the wave arriving at mirror 2 is

$$W(2) = \frac{\epsilon}{2} \int_{-a}^{a} \int_{-a}^{a} |E(2)|^2 \, dx\, dy$$

The fractional diffraction loss per reflection is

$$\alpha_D = \frac{W(1) - W(2)}{W(1)} = 1 - |\sigma_m \sigma_n|^2 \qquad (2\text{-}24)$$

using equation (2-23).

The diffraction losses for various modes are shown in Figure 4. The losses decrease with increasing Fresnel number, as

expected, and are very low for $N \gtrsim 1$. Note that TEM_{uvq} and TEM_{vuq}, $u \neq v$, have the same losses, as can be seen from equations (2-24) and (2-21). In Figure 4 a vertical line is drawn arbitrarily at N = 1 and the loss for each mode is marked by a dotted line. Note that starting with the dominant TEM_{ooq} mode, the loss increases considerably each time we move to a higher order mode.

Spot Size at the Mirrors

From equations (2-19) and (2-20) we can write

$$F_m(c, n_x)\, G_n(c, n_y) = A_m A_n\, H_m\,(\sqrt{c}\, n_x)\, H_n\,(\sqrt{c}\, n_y)\, e^{-\frac{c}{2}(n_x^2+n_y^2)} \qquad (2\text{-}25)$$

The dominant mode (m=n=o) is then

$$F_o(c, n_x)\, G_o(c, n_y) = (A_o)^2\, e^{-\frac{a^2 k}{2b}\,(x^2/a^2 + y^2/a^2)} \qquad (2\text{-}26)$$

Let $w^2 = x^2 + y^2$. Then a spot size at the mirrors can be defined such that at the edge of the spot the dominant mode field is e^{-1} times its value at the center of the mirror. The radius w_s of this spot is given by, from equation (2-26),

$$w_s^2 = \frac{2b}{k}$$

or,

$$w_s = \sqrt{b\lambda/\pi} \qquad (2\text{-}27)$$

So while increasing the mirror dimension a will decrease diffraction losses, the spot size will be unaffected. With b = 100 cm and

$\lambda = 7 \times 10^{-4}$ cm, equation (2-27) gives $w_s = 1.5$ mm.

Polarization

We have considered only electric field patterns which are linearly polarized. However, if a TEM_{01q} mode linearly polarized in the x direction is superimposed on a TEM_{10q} mode linearly polarized in the y direction, the lowest order circular electric mode may result (5, 12). Many other field configurations may be synthesized this way, assuming there is no preferred direction of polarization.

Z-Dependence of the Resonator Field

Traveling-Wave Field

We have obtained the field distributions of the normal modes of the confocal resonator at the mirrors; now we would like to obtain an expression for the field at an arbitrary constant-Z plane (see Figure 2) which may be inside the resonator, or outside, if the transmission of the mirror is accounted for. The field over such a plane caused by the field at one of the mirrors can be found by applying the Huygens-Fresnel principle, using the Hermite-Gaussian eigenfunction approximations for the field at the mirror. The integral can then be evaluated for $c \rightarrow \infty$, and it has been shown that

the traveling wave field of the confocal resonator due to the field at one of the mirrors is (5)

$$\frac{E(x,y,z)}{E_o} = A_m A_n \sqrt{\frac{2}{1+\zeta^2}}\, H_m\left(X\sqrt{\frac{2}{1+\zeta^2}}\right) H_n\left(Y\sqrt{\frac{2}{1+\zeta^2}}\right)$$

$$\cdot \exp\left[\frac{-kw^2}{b(1+\zeta^2)}\right] \exp\left\{-i\left[k\left(\frac{b}{2}(1+\zeta) + \frac{\zeta}{1+\zeta^2}\frac{w^2}{b}\right)\right.\right.$$

$$\left.\left. -(1+m+n)\left(\frac{\pi}{2} - \phi\right)\right]\right\} \qquad (2\text{-}28)$$

where $w^2 = x^2 + y^2$, $\zeta = \frac{2z}{b}$, $\phi = \tan^{-1}\frac{(1-\zeta)}{(1+\zeta)}$

If one of the mirrors is not perfectly reflecting, there will be a transmitted wave with a field given by equation (2-28), but reduced by the mirror transmission coefficient. The field inside the resonator will be a standing wave.

Constant Phase Surfaces

We would like to find the surface intersecting the z axis at $z = z_o$ over which the phase of the confocal field is a constant. The phase angle at the point z_o on the z axis is a constant, say c_1. Then from equation (2-28) we can write

$$\frac{kb}{2}(1+\zeta_o) - (1+m+n)(\pi/2 - \phi) = c_1$$

or,

$$\frac{b}{2}\zeta_o = c_2 \qquad (2\text{-}29)$$

where

$$c_2 = \frac{1}{k}\left[c_1 + (1+m+n)(\pi/2 - \phi) - \frac{kb}{2}\right] \quad \text{and} \quad \zeta_o = \frac{2z_o}{b}$$

Now, at a point (x, y, z) on the constant phase surface the phase is, neglecting the slow variation of ϕ with respect to Z, approximately

$$\frac{b}{2}\zeta + \frac{\zeta_o}{1+\zeta_o^2}\frac{w^2}{b} = c_2 \qquad (2\text{-}30)$$

Subtracting (2-29) from (2-30) gives

$$z - z_o = -\frac{\zeta_o}{1+\zeta_o^2}\frac{w^2}{b} \qquad (2\text{-}31)$$

The surface given by (2-31) is approximately spherical (see Appendix 2). The radius of curvature of this surface is equal to the radius of curvature of the line in the x-z plane defined by equation (2-31) with y = o:

$$z - z_o = -\frac{\zeta_o}{1+\zeta_o^2}\frac{x^2}{b} \qquad (2\text{-}32)$$

So the radius of curvature b' of the constant phase surface intersecting the z-axis at $z = z_o$ is (27)

$$b' = \frac{\left[1+\left(\frac{dz}{dx}\right)^2\right]^{3/2}}{\frac{d^2z}{dx^2}} = \frac{\left[1+\left(\frac{\zeta_o}{1+\zeta_o^2}\right)^2\left(\frac{2x}{b}\right)^2\right]^{3/2}}{\frac{-2\zeta_o}{b(1+\zeta_o^2)}}$$

or

$$b' \cong -\frac{b(1+\zeta_o^2)}{2\zeta_o} \qquad (2\text{-}33)$$

Since we are interested only in $x \ll b$. Note that when ζ_o is positive, b' is negative, and when ζ_o is negative, b' is positive. Since

positive b' means the surface is concave upward and negative b' means the surface is concave downward (27), all of the constant phase surfaces are concave toward the z = o plane (see Figure 5). Having noted this, we can find the magnitude of b' from

$$b' = b \left| \frac{1+\zeta_o^2}{2\zeta_o} \right| \qquad (2\text{-}34)$$

For $\zeta_o = \pm 1$, b' = b, and the constant phase surfaces coincide with the mirrors. Note that, from equation (2-31), the z = o plane is a constant phase surface. Also, the factor $\frac{1+\zeta_o^2}{2\zeta_o}$ in (2-34) is minimized at $\zeta_o = \pm 1$, so the minimum value of b' is b, the confocal radius of curvature.

Spot Size at Arbitrary Z

The spot size at an arbitrary plane $z = z_o$ can be defined such that at the edge of the spot the first exponential term in equation (2-28) falls to e^{-1}. The radius w_s' of this spot is

$$w_s' = \sqrt{\frac{b\lambda\,(1+\zeta_o^2)}{2\pi}} \qquad (2\text{-}35)$$

w_s' is a minimum at z = o, the symmetry plane (see Figure 5).

Symmetry of Modes (5, 6)

We have shown that a confocal resonator of spacing b generates a set of constant phase surfaces of radius of curvature b' given by equation (2-34). Now since these constant phase surfaces are

spherical, then equation (2-28) also gives the field between two spherical mirrors of arbitrary spacing. In other words, any two constant phase surfaces may be replaced by mirrors which fit the constant phase surfaces. The resonant frequencies of the new resonator so formed will be determined by requiring that the round trip phase shift be equal to an integral multiple of 2π .

Consider two identical spherical mirrors of radius of curvature b' separated by a distance d. Then, from equation (2-34) with $\zeta_o = \frac{2z_o}{b} = \frac{d}{b}$, we have

$$b' = b \frac{(1 + d^2/b^2)}{2d/b}$$

or

$$d^2 - 2db' + b^2 = 0 \qquad (2\text{-}36)$$

For a given b and b' there are two possible mirror separations:

$$d_{1,2} = b' \pm \sqrt{b'^2 - b^2} \qquad (2\text{-}37)$$

That is, the mirrors can be placed symmetrically about the $z = o$ plane with a distance d_1 between them or a distance d_2 between them, and in each case the mirrors will coincide with constant phase surfaces. The normal modes of these new resonators will be symmetric about the xy plane which passes through the center of the resonator, which is the $z = o$ plane in this instance.

A resonator which will have mode patterns that are asymmetric about the resonator center can be constructed by

placing one mirror at $z = d_1/2$ and the other mirror at $z = \frac{-d_2}{2}$. The spacing of these two mirrors is, using (2-37),

$$d = \frac{d_1}{2} + \frac{d_2}{2} = b' \tag{2-38}$$

which is their radius of curvature. So this is a "new" confocal system, since the spacing equals the mirror radius of curvature. Now since the new resonator is not symmetric about the center of the generating confocal system (the $z = o$ plane), then the mode patterns of the new resonator are asymmetric about the center of the new resonator.

This asymmetry can be demonstrated by spot size considerations. The dominant mode of the generating confocal system has a spot size w_o at the resonator center given by equation (2-35) with $\zeta_o = o$:

$$w_o = \sqrt{\frac{b\lambda}{2\pi}} \tag{2-39}$$

Then the spot size at a distance $z = d/2$ from the resonator center is, from equations (2-35) and (2-39),

$$w_s' = w_o \sqrt{1 + d^2/b^2} \tag{2-40}$$

So the spot sizes on the mirrors of the new confocal system are

$$\begin{aligned} w_1 &= w_o \sqrt{1 + d_2^2/b^2} \\ w_2 &= w_o \sqrt{1 + d_2^2/b^2} \end{aligned} \tag{2-41}$$

Since the mirrors have different spot sizes, and the minimum spot size is at $z = o$, which is not the center of the new resonator, we

can conclude that the mode patterns of the new confocal system are asymmetric about the resonator center. Note that, using equations (2-37) and (2-41),

$$w_1 w_2 = \frac{\lambda b'}{\pi} \qquad (2\text{-}42)$$

where $\frac{\lambda b'}{\pi}$ would be the mirror spot size for a symmetric set of modes of the new confocal system.

If the mirror radius of curvature b' is fixed, then from equation (2-37) b can be varied to obtain many different sets of d_1 and d_2, and from each set we can devise a confocal resonator. The modes of each of these resonators will have different symmetries, and so it seems that there is not a unique set of modes for a given confocal resonator. This is true, in fact, for a lossless resonator. This discussion of mode symmetry is based on equation (2-28). Recall that (2-28) was obtained in the limit $c \to \infty$. Since $c = 2\pi \frac{a^2}{b\lambda}$, this may be interpreted as requiring that the mirrors have an infinite cross-section, in which case there would be no diffraction losses. However, the mirrors are actually finite in size, so there are diffraction losses which select one of the mode sets. Since the mirrors have identical cross-sections, 2a by 2a, it seems reasonable that the mode set having lowest diffraction losses would be the set characterized by equal spot sizes on the mirrors, and this is the mode set observed in practice. It is important to remember that equation (2-28) gives the field of a lossless confocal resonator.

Beamwidth and Resonator Q

Beamwidth

The angular beamwidth of the TEM_{ooq} mode can be found as follows (5). Form the ratio of the half-power spot size to the distance z_o from the resonator center. Twice the limit of this ratio of $z_o \to \infty$ is equal to the half-power angular beamwidth θ. So from equation (2-35)

$$\theta = 2 \lim_{z_o = \infty} \sqrt{\frac{\ln 2}{2}} \sqrt{\frac{b\lambda \left(1 + \frac{4 z_o^2}{b^2}\right)}{2\pi}} \Big/ z_o$$

Since the half-power spot size is $\sqrt{\frac{\ln 2}{2}}\, w_s'$. This yields

$$\theta = 2\sqrt{\frac{\ln 2}{\pi}}\sqrt{\frac{\lambda}{b}} = .939\sqrt{\frac{\lambda}{b}} \text{ radians} \qquad (2\text{-}43)$$

With $\lambda = 7 \times 10^{-5}$ cm and b = 50 cm, we find $\theta \simeq 10^{-3}$ radians.

Resonator Q

The quality factor Q of a resonator is defined as

$$Q = \omega_o \frac{W}{P} \qquad (2\text{-}44)$$

where ω_o is the resonant radian frequency, W is the time average energy stored in the resonator, and P is the energy loss per second of the resonator. Suppose a normal mode wave is bouncing back and forth between the resonator mirrors (5). There will be some energy

storage W. The curvature of the normal mode phase fronts is small and the phase fronts are approximately planar. Then the energy storage W is approximately uniform over the length d of the resonator, and the energy storage per unit length is W/d. The energy per second passing an equiphase surface is $\frac{cW}{d}$, where c is the velocity of propagation. If α is the fractional power loss per bounce caused by diffraction and reflection losses, the energy loss per second is

$$P = \frac{\alpha c W}{d}$$

Therefore,

$$Q = \frac{\omega_o d}{\alpha c} = \frac{2\pi d}{\alpha \lambda_o}$$

Since $\omega_o/c = 2\pi/\lambda_o$. For a confocal resonator with a reasonably large Fresnel number, the diffraction losses are negligible compared to reflection losses (see Figure 4). If the loss coefficient of a dielectric mirror is .5 percent, then $\alpha = .005$. Suppose the resonator length d is 100 cm, and $\lambda_o = 10^{-4}$ cm. Then

$$Q = \frac{2\pi(100)}{5 \times 10^{-7}} = 1.25 \times 10^9$$

Since α caused by reflection losses does not vary with spacing d, the Q will increase with increasing d until diffraction losses become appreciable. Then α will depend on d, and increasing diffraction losses will decrease the Q as d increases.

A measure of Δf, the half-power bandwidth of the resonance is given by

$$\Delta f = \frac{f_o}{Q} \tag{2-45}$$

where f_o is the center frequency of the resonance. Using the expression for Q we have

$$\Delta f = \frac{a\,c}{2\pi d} \tag{2-46}$$

with $a = .005$, $c = 3 \times 10^{10}$ cm per second, and $d = 100$ cm, this gives

$$\Delta f = .24 \text{ mc}$$

However, if this resonator is used as a laser resonator, the line width will be much smaller than .24 mc. As an analogy consider a one megacycle RF oscillator with a tank circuit Q of 400. For this oscillator

$$\Delta f = \frac{f_o}{Q} = \frac{10^6}{4 \times 10^2} = 2.5 \text{ kc}$$

Certainly the linewidth of the RF oscillations is expected to be much less than 2.5 kc. This writer has observed a secondary standard RF oscillator which had a short term linewidth of 2 cps. Similarly the linewidth of the laser oscillations is expected to be much less than .24 mc. A gas laser oscillating at about 10^{14} cps has been observed to have a short term linewidth of 2 cps (17).

Note that for the confocal case $Q \propto b/\lambda$ (for fixed a) while beamwidth $\theta \propto \sqrt{\lambda/b}$. Therefore an increase in Q will cause a corresponding decrease in beamwidth.

THE NONCONFOCAL RESONATOR

Resonator with Mirrors Having Equal Radii of Curvature

Equivalent Confocal Resonator Analysis (5)

Let us investigate the properties of a resonator consisting of two identical spherical mirrors of radius of curvature b' separated by a distance d. Now we have shown that a confocal resonator generates a family of constant phase surfaces of varying radii of curvature and that a new resonator can be formed by placing spherical mirrors with proper radii of curvature at any two constant phase surfaces. Therefore, a nonconfocal resonator, characterized by the parameters b' and d, may be discussed in terms of an equivalent confocal resonator, characterized by the parameter b, where b, b', and d are linked by equation (2-36). For given values of b' and d, equation (2-36) can be solved for the required value of b. This yields

$$b = \sqrt{d}\ \sqrt{2b'-d} \qquad (3-1)$$

So for this analysis to be meaningful, b' and d must be chosen such that $b' \geq d/2$; this condition limits this analysis to resonators for which mirror spacing is concentric or closer.

Spot Size at the Mirrors. The spot size at the mirrors of the nonconfocal resonator can be found using equation (2-35), with

$\zeta_o = d/b$, and equation (3-1):

$$w_s'^2 = \frac{\lambda\sqrt{2db'-d^2}\left(1 + \frac{d^2}{2db'-d^2}\right)}{2\pi}$$

or,

$$w_s' = \sqrt{\frac{\lambda d}{\pi}}\left[2\frac{d}{b'} - \left(\frac{d}{b'}\right)^2\right]^{-1/4} \qquad (3-2)$$

If the factor in brackets in equation (3-2) is maximized with respect to b', the maximizing value of b' is d and the maximum value of the term is one. So for a given spacing d, the mirror spot size is a minimum when the mirror radii of curvature equal the spacing, i.e., for the confocal case. Note that the idea of an equivalent confocal resonator does not apply to plane-parallel mirror resonators, since, from equation (3-2), if $b' \to \infty$ for fixed d, then the spot size w_s' increases without bound.

Diffraction Loss. Suppose a nonconfocal resonator has mirrors of square cross-section 2a' on a side. Now the equivalent confocal resonator, characterized by the parameter b, of which we have been speaking is a lossless resonator. However, the losses of the nonconfocal resonator can be estimated as follows (5). Assume that the loss of the nonconfocal resonator is equal to that of its equivalent confocal resonator, not with infinite mirrors, but with mirrors of square cross-section 2a by 2a, where

$$2a = 2a'\frac{w_s}{w_s'} \qquad (3-3)$$

That is, we assume that the mirrors of the equivalent confocal

resonator are smaller than those of the nonconfocal resonator by a factor $\frac{w_s}{w'_s}$. Using equations (2-27), (2-36) and (3-2), we can write

$$2a = \frac{2a' \left[\frac{\lambda \sqrt{2db' - d^2}}{\pi}\right]^{1/2} \left[\frac{2d}{b'} - (d/b')^2\right]^{1/4}}{\sqrt{\frac{\lambda d}{\pi}}}$$

$$= 2a' (2 - d/b')^{1/2} \qquad (3-4)$$

Now the Fresnel number of the equivalent confocal resonator is, using equations (3-1) and (3-4),

$$\frac{a^2}{b\lambda} = \frac{a'^2(2-d/b')}{\lambda \sqrt{db'}\sqrt{2-d/b'}} = \frac{a'^2}{d\lambda} \left[2\, d/b' - (d/b')^2\right]^{1/2} \qquad (3-5)$$

As Fresnel number increases, diffraction losses decrease. Equation (3-5) is maximized as a function of b' by b' = d. So for a given spacing d the confocal case gives minimum loss.

Note that this equivalent confocal resonator analysis gives accurate results only if the mirrors of the nonconfocal resonator intercept most of the confocal field. Otherwise the fields in the nonconfocal resonator are not approximately given by equation (2-28). An equivalent requirement is that the nonconfocal mirror dimension a' must be somewhat larger than the spot size w'_s at the mirror. So from equation (3-2) we require that

$$\frac{a'^2}{d\lambda} > \frac{1}{\pi} \left[2d/b' - (d/b')^2\right]^{-1/2} \qquad (3-6)$$

Mode Volume. The mode volume V can be defined as the area of the spot at the reflector times the reflector spacing (5). Using

equation (3-2), we have

$$V = \pi w_s'^2 d = \lambda d^2 \left[2d/b' - (d/b')^2 \right]^{-1/2} \qquad (3\text{-}7)$$

If a spherical mirror resonator is used as a laser resonator, the mode volume is a measure of the required volume of the active medium. The volume V is a minimum for d = b', the confocal case.

Resonance Condition. The resonance condition of the nonconfocal resonator can be obtained from equation (2-28). The mirrors are placed at $\pm d/2$, and the phase at $\pm d/2$ is

$$P(\pm d/2) = k(b/2 \pm d/2) - (1+m+n)\left[\pi/2 - \tan^{-1}\left(\frac{b \mp d}{b \pm d}\right)\right] \qquad (3\text{-}8)$$

Then the phase difference between the mirrors is

$$P(+d/2) - P(-d/2) = kd - (1+m+n)\left[\frac{\pi}{2} - \tan^{-1}\left(\frac{b-d}{b+d}\right) - \frac{\pi}{2} + \tan^{-1}\left(\frac{b+d}{b-d}\right)\right] \qquad (3\text{-}9)$$

Since $(\pi/2 - x) = \cot^{-1}(\tan x)$, equation (3-9) can be written

$$P(+d/2) - P(-d/2) = kd - (1+m+n)\left[\pi/2 - 2\tan^{-1}\left(\frac{b-d}{b+d}\right)\right] \qquad (3\text{-}10)$$

At resonance, the round trip phase shift must be $2\pi q$, $q = 1, 2, \ldots$. So equation (3-10) becomes

$$2\pi q = 2kd - (1+m+n)\left[\pi - 4\tan^{-1}\left(\frac{b-d}{b+d}\right)\right]$$

or,

$$\frac{4d}{\lambda} = 2q + (1+m+n)\frac{2}{\pi}\left[\frac{\pi}{2} - 2\tan^{-1}\left(\frac{b-d}{b+d}\right)\right] \qquad (3\text{-}11)$$

Using equation (2-36) and noting that $\pi/2 - 2x = \cos^{-1}\left[2\tan x/(1+\tan^2 x)\right]$, equation (3-11) becomes (6)

$$\frac{4d}{\lambda} = 2q + \frac{2}{\pi}(1+m+n)\cos^{-1}(1-d/b') \qquad (3\text{-}12)$$

So for the nonconfocal case $\frac{4d}{\lambda}$ is not necessarily an integer, and also the modes are no longer degenerate in (m+n) and q.

Resonator with $d \gg b$ (36)

Let us investigate the properties of an identical mirror resonator with highly nonconfocal spacing, i.e., $d \gg b$, where d is the spacing and b is the radius of curvature of the mirrors. Since the mirrors are identical, the normal modes may be found by applying the "single-pass" equation (2-1), requiring that $E'(x', y') = \sigma_m \sigma_n E(x', y')$. Assume that $E(x, y) = E_o f_m(x)\, g_n(y)$ and that d/b is large enough so that

$$\frac{d-b}{2bd}\ (x_1^2 + x'^2) \gg \frac{x_1 x'}{d} \qquad (3\text{-}13)$$

with a similar expression for y. This resonator is identical to the one shown in Figure 2, except for the spacing d. Then using equations (2-1), (2-7), and (3-13) we can write

$$\sigma_m \sigma_n f_m(x')\, g_n(y') = \frac{ik}{2\pi d} \int_{-a}^{a} \int_{-a}^{a} f_m(x_1)\, g_n(y_1) \cdot e^{-ikd}\, e^{ik \frac{d-b}{2bd} (x_1^2 + x'^2 + y_1^2 + y'^2)}\, dx_1\, dy_1 \qquad (3\text{-}14)$$

In terms of variables defined earlier equation (3-14) becomes (since $d \gg b$)

$$\sigma_m \sigma_n F_m(X')\, G_n(Y') = \frac{i\, e^{-ikd}}{2\pi} \int_{-\sqrt{c}}^{\sqrt{c}} \int_{-\sqrt{c}}^{\sqrt{c}} F_m(X_1)\, G_n(Y_1) \cdot e^{\,i \frac{d}{2b} (X_1^2 + X'^2 + Y_1^2 + Y'^2)}\, dX_1\, dY_1 \qquad (3\text{-}15)$$

Equation (3-15) can be written as two equations of the same form, so consider one of them:

$$\sigma_m F_m(X') = \frac{e^{i\pi/4}\, e^{-ikd/2}}{\sqrt{2\pi}}\; e^{i\frac{d}{2b}X'^2} \int_{-\sqrt{c}}^{\sqrt{c}} F_m(X_1)\, e^{i\frac{d}{2b}X_1^2}\, dX_1 \qquad (3\text{-}16)$$

The integral term in equation (3-16) is independent of X' and can be represented by a constant A_1. So equation (3-16) becomes

$$\sigma_m F_m(X') = \frac{A_1 e^{i(\pi/4 - kd/2)}}{\sqrt{2\pi}}\; e^{i\frac{d}{2b}X'^2} \qquad (3\text{-}17)$$

and because of symmetry we can write

$$\sigma_m F_m(X_1) = \frac{A_1\, e^{i(\pi/4 - kd/2)}}{\sqrt{2\pi}}\; e^{i\frac{d}{2b}X_1^2} \qquad (3\text{-}18)$$

Now solve (3-18) for $F_m(X_1)$, and put that result in the integral of (3-16). Then equate the right side of (3-16) to the right side of (3-17). This procedure yields

$$\sigma_m = \frac{e^{i(\pi/4 - kd/2)}}{\sqrt{2\pi}} \int_{-\sqrt{c}}^{\sqrt{c}} e^{i\frac{d}{b}X_1^2}\, dX_1 \qquad (3\text{-}19)$$

The integral in (3-19) can be evaluated for $c \to \infty$.

$$\sigma_m = \frac{e^{i(\pi/4 - kd/2)}}{\sqrt{2\pi}}\; \frac{\sqrt{\pi}}{\sqrt{d/b}}\; e^{-i3\pi/4} = \frac{-e^{-ikd/2}}{\sqrt{2d/b}} \qquad (3\text{-}20)$$

The fractional diffraction loss is

$$\alpha_D = 1 - |\sigma_m \sigma_n|^2 = 1 - \left(\frac{b}{2d}\right)^2 \qquad (3\text{-}21)$$

This high diffraction loss (e.g., d/b = 5 gives $\alpha_D = .99$) is plotted in Figure 7.

Now, using equations (3-18) and (3-19), we can write

$$\frac{1}{F_m(X_1)} \; A_1 \, e^{i \frac{d}{2b} X_1^2} = \int_{-\sqrt{c}}^{\sqrt{c}} e^{i \frac{d}{b} X_1^2} \; dX_1$$

So,

$$F_m(X) \propto e^{i\, d/2b\, X^2} \tag{3-22}$$

and the solution to equation (3-15) is

$$F_m(X)\, G_n(Y) \propto e^{i \frac{d}{2b}(X^2 + Y^2)}$$

Therefore,

$$f_m(x)\, g_n(y) \propto e^{i \frac{k}{2b}(x^2 + y^2)} \tag{3-23}$$

The field magnitude (and therefore the energy density) is constant over the mirrors and the phase variation is given by equation (3-23). For $\lambda = 10^{-4}$ cm and b = 100 cm, the phase difference between the mirror center and the circle of radius .1 cm centered on the resonator axis is π radians. Because we have assumed an $e^{j\omega t}$ time dependence (see Appendix 1), equation (3-23) indicates that there are inward traveling waves along the mirror surface. This can be seen by considering plane waves passing a reference plane, as shown in Figure 6. A plane wave of wavelength λ and group velocity (which is defined as the velocity of energy transport) v_g is incident on the reference plane at an angle θ. The phase shift per centimeter across the surface of the reference plane is given by $\Delta\phi/\text{cm} = \frac{2\pi \sin\theta}{\lambda}$. This wave may be resolved into two waves, one incident normally to the surface with group velocity $v_g \cos\theta$, and one travelling parallel to the surface with group velocity $v_g \sin\theta$. Then a non-zero phase shift per

unit length ($\Delta\phi$/cm) over the surface means that there is energy propagated parallel to the surface.

From equation (3-23) $\Delta\phi$/cm across the mirror surface is $\frac{\Delta\phi}{\text{cm}} = \frac{d}{dw}\left(\frac{\pi w^2}{b\lambda}\right) = \frac{2\pi}{b\lambda} w$, where $w^2 = x^2 + y^2$. At the mirror center $\frac{\Delta\phi}{\text{cm}}$ is zero, and the wave is incident normally. As we move away from the mirror center, $\frac{\Delta\phi}{\text{cm}}$ increases, and the wave must be incident at some non-zero angle θ. Consider Figure 15(a). The mirror M_2 is far from the other mirror (since $d \gg b$), and so the wave incident on M_2 is approximately a spherical traveling wave. At a point away from the mirror center $\Delta\phi$/cm is non-zero and the wave incident at the point can be resolved into a normal component, with group velocity v_n, and a parallel component, with group velocity v_p. The group velocity v_p decreases to zero as we approach the mirror center, because the field is normally incident there. The vector sum of v_n and v_p is the same for each point on the surface, because of the spherical nature of the incident traveling wave. We can gain insight into the nature of the large loss by using geometrical optics. The normal components will be reflected back through the mirror center of curvature, as shown in Figure 15(b), and those normal components which are reflected from points outside the region A will miss the other mirror. Consequently, when $d \gg b$, what we have called diffraction loss really includes energy loss resulting from

the geometry of the system as well as diffraction loss.

As a contrast to the $d \gg b$ case, consider the confocal case, as shown in Figure 15(c). The phase shift per unit length over the confocal mirrors is essentially zero (see Appendix 2). Therefore, the wave traveling parallel to the mirror surface is negligible, and the field is normally incident over the mirrors. The normal components are reflected back to the mirror center of curvature which lies at the center of the other mirror. Because of this strong focussing action, there is no loss predicted by geometrical optics as there is in the $d \gg b$ case, and we expect diffraction losses to be small, which they are.

Arbitrary Spacing

A resonator with arbitrary mirror spacing can be investigated by solving for the eigenfunctions of equation (2-1) using equation (2-7) without the approximation (3-13). This has been done (36) by numerical methods. The diffraction loss $\alpha_D = 1 - |\sigma_m \sigma_n|^2$ is plotted in Figure 7 as a function of d/b, for $c = 5/(d/b)$. At confocal spacing, $c = 2\pi \frac{a^2}{b\lambda}$, so $a^2 = \frac{5}{2} \frac{b\lambda}{\pi}$, but $\sqrt{\frac{b\lambda}{\pi}}$ is the spot size at the confocal mirrors. So $a = \sqrt{\frac{5}{2}}\ w_s$, and at confocal spacing the mirror dimension a is larger than the spot size by a factor of $\simeq 1.6$. It is seen from Figure 7 that α_D is a minimum for confocal spacing, as expected. The diffraction loss begins to rise very rapidly as

$d/b \rightarrow 2$, which is concentric spacing. Equation (3-21) is fairly accurate for $d/b > 6$.

Resonator with Mirrors Having Unequal Radii of Curvature

Equivalent Confocal Resonator Analysis (6)

A general nonconfocal resonator is one consisting of two spherical mirrors M_1 and M_2 with different radii of curvature b_1 and b_2, separated by a distance d. We can discuss this resonator in terms of an equivalent confocal resonator. A resonator can be formed by placing the mirrors in the confocal field, given by equation (2-28), at such positions that they coincide with constant phase surfaces. Then, using equation (2-36), mirror M_1 can be placed at $\pm d_{1/2}$ and mirror M_2 at $\pm d_{2/2}$, where

$$d_1 = b_1 \pm \sqrt{b_1^2 - b^2}$$
$$d_2 = b_2 \pm \sqrt{b_2^2 - b^2} \qquad (3\text{-}24)$$

So with a given pair of mirrors, four distinct resonators can be constructed that will fit the constant phase surfaces. The mirror separation for each of these resonators is

$$d = \frac{d_1}{2} + \frac{d_2}{2} = \frac{1}{2}\left(b_1 + b_2 \pm \sqrt{b_1^2 - b^2} \pm \sqrt{b_2^2 - b^2}\right) \qquad (3\text{-}25)$$

Other resonators can be obtained by varying the confocal parameter b, but its range of variation is restricted due to the radical terms in (3-25). If $b_2 > b_1$, then b can range only from 0 to b_1, and

this in turn restricts the range of values of d. This may be seen by solving equation (3-25) for b. The result is

$$b^2 = \frac{-x^4 - (b_1^2 - b_2^2)^2 + 2x^2 (b_1^2 + b_2^2)}{4x^2}$$

where $x = (2d - b_1 - b_2)$. After simplification this becomes

$$b^2 = \frac{4d\,[(b_1 - d)(b_2 - d)(b_1 + b_2 - d)]}{(b_1 + b_2 - 2d)^2} \qquad (3\text{-}26)$$

Then, from (3-26), since b must be real, d is limited to $o < d < b_1$ and $b_2 < d < b_1 + b_2$. This can be expressed differently by writing equation (3-26) in terms of the parameters g_1 and g_2, where (11)

$$g_1 = 1 - d/b_1$$
$$g_2 = 1 - d/b_2 \qquad (3\text{-}27)$$

In terms of g_1 and g_2, (3-26) becomes (18)

$$b^2 = \frac{4d^2\, g_1 g_2\, (1 - g_1 g_2)}{(g_1 + g_2 - 2g_1 g_2)^2} \qquad (3\text{-}28)$$

From equation (3-28), if b is to be real, then

$$o \leq g_1 g_2 \leq 1 \qquad (3\text{-}29)$$

It has been shown (6) by an argument based on an equivalent sequence of lenses that (3-29) is a diffraction loss condition; resonators which obey (3-29) are low loss, or stable resonators, while resonators which violate (3-29) are high loss, or unstable resonators.

Equation (3-5) may be rewritten as (11)

$$\frac{a^2}{b\lambda} = \frac{a'^2}{d\lambda}\,[1 - g^2]^{1/2} \qquad (3\text{-}30)$$

where $g = g_1$ or g_2. Now if a nonconfocal resonator is stable and if

the nonconfocal mirrors intercept most of the confocal field, then using (3-30) we can compute the Fresnel number $\frac{a^2}{b\lambda}$ of an equivalent confocal resonator and obtain an estimate of the diffraction losses of the nonconfocal resonator. Otherwise we cannot say what the losses are, except that they are "high."

Loss Diagram

The stability condition $o \leq g_1 g_2 \leq 1$ can be represented by a two-dimensional plot with g_1 and g_2 as axes (11), as in Figure 8. Any given resonator is represented on this loss diagram by a single point. The cross-hatched area is the high loss area. The origin represents the confocal resonator with mirrors of equal curvature. Note that deviations from the ideal confocal dimensions $d = b_1 = b_2$ could cause high loss in a confocal resonator. Operating points should be chosen at a safe distance from the high loss region (6). All resonators with mirrors of equal curvature lie on the line $g_1 = g_2$. Note that there are no convex-convex systems in the low loss region.

A transition from the low loss region to the high loss region means a sharp increase in diffraction loss, for large values of the Fresnel number N (6). While losses of resonators lying in the stable region can be estimated using equation (3-32), no similar estimate of losses in the unstable region can be made. For very large N, the crosshatched regions in the loss diagram are areas of

essentially 100 percent loss due to diffraction. However, for smaller N, the transition from the stable region to the unstable region is not so sharp (11), and stable modes may exist for large N resonators which do not lie too far into the unstable region (33).

Resonance Condition

The resonance condition for a resonator with mirrors spaced at a distance d and having radii of curvature b_1 and b_2 can be obtained from equation (2-28) as (6)

$$\frac{4d}{\lambda} = 2q + \frac{2}{\pi}(1+m+n)\cos^{-1}\sqrt{(1-d/b_1)(1-d/b_2)}$$

or,

$$\frac{2d}{\lambda} = q + \frac{1}{\pi}(1+m+n)\cos^{-1}(g_1g_2)^{1/2} \qquad (3\text{-}31)$$

Note that equation (3-31) reduces to equation (3-12) when $b_1 = b_2$.

A half nonconfocal resonator (6) may be constructed by placing a spherical mirror having radius of curvature b_1 at a distance d from a plane mirror, if $d \leq b_1$. The resonance condition for this resonator can be obtained by taking $b_2 \rightarrow \infty$ in equation (3-31) because the radius of curvature of a plane mirror is infinite. This yields, since $\theta = \frac{1}{2}\cos^{-1}(2\cos^2\theta - 1)$,

$$\frac{4d}{\lambda} = 2q + \frac{1}{\pi}(1+m+n)\cos^{-1}(1 - 2d/b_1) \qquad (3\text{-}32)$$

Note that if $d = b_1$, equation (3-32) reduces to equation (2-22), the resonance condition of the confocal resonator.

MODE SELECTION

Interaction Between Normal Modes and Active Medium

It has been shown that the normal modes of oscillation of a spherical mirror optical resonator may be labeled as TEM_{mnq}, where m and n refer to field variations in the x and y directions and q is the number of half wavelengths in the standing wave pattern between the mirrors.[1] The frequencies of these modes for a general nonconfocal resonator are given by equation (3-31) as

$$f = \frac{c}{2d} [q + (1+m+n)s] \qquad (4\text{-}1)$$

where $s = \frac{1}{\pi} \cos^{-1} (g_1 g_2)^{1/2}$. The factor s varies between zero and one-half for resonators lying in the stable region of the loss diagram. For a given value of q, m or n can take the values 0, 1, 2, ...; i.e., for a given longitudinal mode characterized by a certain value of q there is a set of transverse modes, with each transverse mode characterized by its values of m and n. The frequency difference between two modes having the same sum (m+n) but different q is

$$\Delta f_q = \frac{c}{2d} \Delta q \qquad (4\text{-}2)$$

while the frequency difference between two modes having the same q but different (m+n) is

---

[1] Note that in the optical region q is very large; e.g., if $\lambda = 10^{-4}$ cm and d = 50 cm, then $q = \frac{2d}{\lambda} = 10^6$.

$$\Delta f_{(m+n)} = \frac{c}{2d} \Delta(m+n)\, s \qquad (4-3)$$

A representation of the frequency spectrum is given in Figure 9. There will be varying degrees of degeneracy in the frequency spectrum, depending on the value of the geometrical factor s.

Now in the active medium of a laser, such as a mixture of helium and neon gas, the emission lines are not perfectly sharp. The lines are broadened primarily through a Doppler shift in the frequency of the emitted quanta (10). This Doppler shift is caused by the random thermal motion of the atoms in the active medium. For example, the Doppler broadened width of the 6328 Å transition in the He-Ne laser is about 1500 mc (14). The value of Δf_q for a resonator of length d = 100 cm is 150 mc; so a He-Ne laser using this resonator will in general oscillate in more than one of the resonator's normal modes (24). This is illustrated in Figure 10. The broad envelope curve represents the gain per pass of the active medium as a function of frequency, while the sharp peaked curves each represent a dominant mode (TEM_{ooq}) resonance of the resonator. The horizontal line represents an assumed total loss per pass for these resonances; this is constant since loss does not vary with longitudinal mode order. Oscillations in the resonator can occur in the modes for which the gain exceeds the loss in Figure 10. Note that modes of higher order m and n are omitted from Figure 10. Oscillations occur in some of these modes also, providing the medium gain is sufficient

to overcome their losses. In general a laser oscillates in several different longitudinal and transverse modes, and the laser output contains several different frequencies. The actual number of modes in which oscillations occur depends on the resonator geometry and losses, the width of the emission line, and the gain of the active medium (25). For many applications a single frequency output is desirable (15, 25). To obtain a single frequency output, oscillations must be confined to a single transverse mode and a single longitudinal mode. Several suitable methods of transverse and longitudinal mode selection have been devised and will be discussed here.

Transverse Mode Selection

Among the various loss mechanisms present in an optical resonator, only the diffraction loss varies significantly with transverse mode order. The dominant mode has the lowest diffraction loss of all the transverse modes, and the diffraction losses increase with increasing transverse mode order.

A resonator having a low Fresnel number, such that the mirrors are only slightly larger than the dominant mode spot size, is inherently mode selective (25). This is because the higher order modes have a larger lateral extent than the dominant mode and thus higher diffraction losses than the dominant mode. Then a laser using this low Fresnel number resonator will oscillate only in

the dominant transverse mode, providing the gain of the active medium is not sufficient to overcome the additional losses of the higher order transverse modes. However, a long, thin resonator such as this is undesirable because the number of possible longitudinal resonances increases with increasing resonator length. Also decreasing the mirror size increases the dominant mode diffraction loss and therefore tends to decrease the laser output power capability (25).

A small mirror does not mean decreased power output, however, if diffraction output coupling is used. Usually power is extracted from a laser through a partially transmitting mirror. In diffraction coupling, power is coupled out of the device by collecting the light that is diffracted around a mirror; therefore the diffraction "loss" becomes useful output instead of loss (23). In this case, a very small mirror (which will select the dominant transverse mode) can be used without sacrificing any power output.

Certain high Fresnel number resonators which lie in the unstable region of the loss diagram may be inherently mode selective (33). These resonators have sizable diffraction losses which may cause discrimination among transverse modes. The diffraction losses of many unstable resonators occur at one mirror only. These resonators are well suited for diffraction output coupling. One of these unstable resonators has been used successfully as a laser

resonator, but its mode selection properties were not determined (33).

A simple method (31) of forcing a laser to oscillate in only the dominant transverse mode is to place an aperture (e.g., an absorbing sheet with a circular hole in it) within the resonator and centered on the resonator axis of symmetry (see Figure 11). Since the lateral extent of the modes increases with increasing transverse mode order, a properly chosen aperture will introduce high loss to the higher order transverse modes without appreciably affecting the dominant mode (25).

We have discussed methods of selecting only one transverse mode, the dominant mode. In general, operation in the dominant mode is desirable, because this mode has lowest diffraction losses and smallest beamwidth. However, higher order transverse modes may be selected by using an aperture of variable size (30), by intentionally misaligning the resonator mirrors to utilize their optical irregularities (14, 22), and by placing opaque wires transversely within the resonator (28, 29, 30). The observed transverse field distributions of these higher order modes agree with the predictions of the Hermite-Gaussian functions (equation 2-25).

Longitudinal Mode Selection

Even though a laser is forced to oscillate in only the dominant

transverse mode, the output radiation will not be single frequency. This is because oscillations will occur in several longitudinal modes simultaneously. Adjacent longitudinal modes are separated by a frequency c/2d (from equation (4-2) with $\Delta q = 1$). A straightforward method of forcing a laser to operate in a single longitudinal mode is to employ a resonator which is so short that not more than one of its longitudinal resonances falls under the Doppler-broadened gain curve (15, 16). For example, if the mirror spacing d is 9.5 cm, then the frequency separation between adjacent longitudinal modes is 1580 mc. Then if the laser is a He-Ne type operating on the 6328 Å line (Doppler width 1500 mc), oscillations will occur in only one longitudinal mode, since the oscillation range is approximately equal to the Doppler width of the line (15). Since the gain of the He-Ne active medium is about 10 percent per meter (21), a laser this short is expected to have low gain per pass and may not oscillate. However, the gain of a short He-Ne laser may be increased by using small bore discharge tubes and by using the helium isotope He^3 instead of normal helium (15).

Longitudinal mode selection has also been effected by the addition of extra mirrors to a two-mirror resonator (20, 21). A scheme using three mirrors (21) is illustrated in Figure 12. This resonator consists of a primary cavity, formed by mirrors A and B, and a secondary cavity, formed by mirrors B and C. Interference

effects cause the effective reflection coefficient of the secondary cavity to vary with frequency, and the frequencies for maximum and minimum reflectivity depend critically on the spacing between B and C. Since the gain of the He-Ne active medium is fairly low, a small reduction in reflection coefficient at a certain frequency will prevent oscillation at that frequency. By precisely controlling the position of mirror C and by eliminating higher order transverse modes with an aperture, a single frequency output is obtained.

The plane parallel Fabry-Perot etalon (4) has been used for longitudinal mode selection (8, 32). A configuration using an etalon placed inside a plane mirror[1] resonator (8) is shown in Figure 13. Interference effects in the etalon cause discrimination among longitudinal modes (4). Also, the angular bandpass characteristics of the etalon limits the beamwidth of the laser fields, and thus lower order transverse modes are favored. The angular passband of the etalon decreases as the angle of tilt θ increases. Mode selectors of this type can be designed to give a single frequency output.

It may be possible to decrease the gain of a laser active

---

[1]The normal modes of a plane mirror resonator are characterized by longitudinal and transverse periodicity as are normal modes of a spherical mirror resonator. However, the fields are not concentrated so tightly about the resonator axis and consequently diffraction losses are much higher (12).

medium to the point that oscillations will occur in only one longitudinal mode (17). However, this would limit the available output power.

SUMMARY

We have determined the properties of the Fabry-Perot interferometer with spherical mirrors when used as a resonant structure. The confocal resonator, which consists of two identical mirrors having radii of curvature b spaced at a distance d = b, was considered first. By applying the Huygens-Fresnel principle, it was found that there are normal modes of oscillation in the sense of self-reproducing field distributions over the mirrors. The modes were labeled TEM_{mnq}, where m and n refer to field variations in the directions transverse to the resonator axis and q is the number of half wavelengths in the standing wave pattern between the mirrors. A normal mode is characterized by its field configuration, its diffraction loss, and its oscillation frequency. The diffraction loss increases with increasing m and n, with the dominant (TEM_{ooq}) mode having the lowest diffraction losses. The mode frequencies depend on the mirror spacing d and on the values of m, n, and q. The modes are highly degenerate in frequency.

The magnitude of the dominant mode field drops to e^{-1} times its value at the mirror center at a distance w_s from the center, where w_s is defined to be the spot size. If the mirror half-width a is slightly larger than w_s, the dominant mode diffraction losses are very small, while modes of higher transverse order may have large

losses. The normal modes are linearly polarized; however, degenerate modes may combine to form circularly polarized modes if there is no preferred direction of polarization. For a typical case, the angular beamwidth of the dominant mode of a confocal resonator is 10^{-3} radian, and the Q of the mode resonance is 10^{9}. The Q and the beamwidth are interdependent, with an increase in Q causing a decrease in beamwidth (for fixed losses). When a spherical mirror resonator is used as a laser resonator, this high Q causes the line width of the laser oscillation to be very narrow.

Investigation of the traveling wave field of the confocal resonator revealed that the resonator generates constant phase surfaces which are spherical. Then spherical mirrors can be placed at these constant phase surfaces to form nonconfocal resonators whose properties can be described in terms of an equivalent confocal resonator, as long as the nonconfocal resonator mirrors intercept most of the confocal resonator field. For a given mirror spacing d, the confocal resonator (b=d) has minimum diffraction loss, minimum mode volume, and minimum spot size at the mirrors. A resonator with $d \gg b$ was seen to have large loss. Part of this loss is geometrical loss, in contrast to the confocal case where there is no geometrical loss. A plot of diffraction loss versus d/b illustrated the minimum loss at d/b = 1, the confocal case.

By considering a general resonator with mirrors having radii

of curvature b_1 and b_2 spaced at a distance d, it was shown that resonators satisfying the condition $0 \leq (1-d/b_1)(1-d/b_2) \leq 1$ are stable (low-loss) while all other resonators are unstable (high loss). This stability condition was represented using a two-dimensional loss diagram. A transition from the stable to the unstable region of the loss diagram means a sharp increase in diffraction loss (for resonators having a reasonably high Fresnel number $N = a^2/d\lambda$). The normal modes of nonconfocal resonators in general have a smaller degree of frequency degeneracy than do the confocal resonator modes.

The fact that the emission lines of laser materials are generally broader than the frequency separation between adjacent mode resonances causes lasers using spherical mirror resonators to oscillate in several different modes simultaneously. For many applications a single frequency output is desirable; therefore methods of suppressing unwanted oscillations must be employed. Apertures and opaque wires are effective in discriminating among transverse (m and n) orders. Also, a very small mirror will select the dominant transverse mode, but then diffraction output coupling should be used so as not to reduce power output capability. Unwanted longitudinal (q) orders can be suppressed by using a short resonator, or by adding extra reflecting surfaces to the resonator which suppress unwanted orders through interference effects. The gain of a laser active medium may be made small enough that oscillations are

limited to one longitudinal order; however, output power would then be limited.

BIBLIOGRAPHY

1. Baker, Bevan B. and E. T. Copson. The mathematical theory of Huygens' principle. 2d ed. Oxford, Oxford University Press, 1953. 192 p.

2. Bergstein, Leonard and Harry Schachter. Resonant modes of optic interferometer cavities, I. Plane parallel end reflectors. Journal of the Optical Society of America 54:887-903. 1964.

3. Birnbaum, George. Optical masers. New York, Academic Press, 1964. 306 p.

4. Born, Max and Emil Wolf. Principles of optics. New York, Pergamon Press, 1959. 803 p.

5. Boyd, G. D. and J. P. Gordon. Confocal multimode resonators for millimeter through optical wavelength masers. Bell System Technical Journal 40:489-508. 1961.

6. Boyd, G. D. and H. Kogelnik. Generalized confocal resonator theory. Bell System Technical Journal 41:1347-1369. 1962.

7. Clark, Peter O. A self-consistent field analysis of spherical-mirror Fabry-Perot resonators. Proceedings of the Institute of Electrical and Electronics Engineers 53:36-41. 1965.

8. Collins, S. A. and G. R. White. Interferometer laser mode selector. Applied Optics 2:448-449. 1963.

9. Dettmann, John W. Mathematical methods in physics and engineering. New York, McGraw-Hill, 1962. 323 p.

10. Eisberg, Robert Martin. Fundamentals of modern physics. New York, Wiley, 1961. 729 p.

11. Fox, A. G. and T. Li. Modes in a maser interferometer with curved and tilted mirrors. Proceedings of the Institute of Electrical and Electronics Engineers 51:80-89. 1963.

12. _____. Resonant modes in a maser interferometer. Bell System Technical Journal 40:453-488. 1961.

13. _____. Resonant modes in an optical maser. Proceedings of the Institute of Radio Engineers 48:1904-1905. 1960.

14. Goldsborough, John P. Beat frequencies between modes of a concave-mirror optical resonator. Applied Optics 3:267-275. 1964.

15. Gordon, E. I. and A. D. White. Single frequency gas lasers at 6328 Å. Proceedings of the Institute of Electrical and Electronics Engineers 52:206-207. 1964.

16. Haisma, J. and H. Delang. Mode patterns obtained by tuning a small gas laser. Physics Letters 3:240-242. 1963.

17. Javan, A., E. A. Ballik and W. L. Bond. Frequency characteristics of a continuous wave He-Ne optical maser. Journal of the Optical Society of America 52:96-98. 1962.

18. Karube, N. Calculated divergence of laser beam from generalized spherical mirror cavities. Proceedings of the Institute of Electrical and Electronics Engineers 52:327-328. 1964.

19. Killpatrick, J., H. Gustafson and L. Wold. Alignment characteristics of a helium-neon optical maser. Proceedings of the Institute of Radio Engineers 50:1521. 1962.

20. Kleinman, D. A. and P. P. Kislink. Discrimination against unwanted orders in the Fabry-Perot resonator. Bell System Technical Journal 41:453-462. 1962.

21. Kogelnik, H. and C. K. N. Patel. Mode suppression and single frequency operation in gaseous optical masers. Proceedings of the Institute of Radio Engineers 50:2365-2366. 1962.

22. Kogelnik, H. and W. W. Rigrod. Visual display of optical resonator modes. Proceedings of the Institute of Radio Engineers 50:220. 1962.

23. Latourette, J. T., S. F. Jacobs and P. Rabinowitz. Improved laser angular brightness through diffraction coupling. Applied Optics 3:981-982. 1964.

24. Lengyel, Bela A. Lasers. New York, Wiley, 1962. 125 p.

25. Li, T. Mode selection in an aperture limited concentric maser interferometer. Bell System Technical Journal 42: 2609-2620. 1963.

26. Lovitt, William Vernon. Linear integral equations. New York, Dover Publications, 1950. 253 p.

27. Merritt, Frederick S. Mathematics manual. New York, McGraw-Hill, 1962. 378 p.

28. Okaya, A. Mode suppression on lasers by metal wires. Proceedings of the Institute of Electrical and Electronics Engineers 52:1741. 1964.

29. Polyani, Thomas G. and William R. Watson. Gaseous optical maser with external mirrors. Journal of Applied Physics 34: 553-560. 1963.

30. Rigrod, W. W. Isolation of axi-symmetrical optical resonator modes. Applied Physics Letters 2:51-53. 1963.

31. Rigrod, W. W. et al. Gaseous optical maser with external concave mirrors. Journal of Applied Physics 33:743-744. 1962.

32. Roess, Dieter. Ruby laser with mode selective etalon reflector. Proceedings of the Institute of Electrical and Electronics Engineers 52:196-197. 1964.

33. Siegman, A. E. Unstable optical resonators for laser applications. Proceedings of the Institute of Electrical and Electronics Engineers 53:277-287. 1965.

34. Silver, Samuel (ed.) Microwave antenna theory and design. New York, McGraw-Hill, 1949. 623 p.

35. Slepian, D. and H. O. Pollak. Prolate spheroidal wave functions, Fourier analysis, and uncertainty - I. Bell System Technical Journal 40:43-63. 1961.

36. Soohoo, R. F. Nonconfocal multimode resonators for lasers. Proceedings of the Institute of Electrical and Electronics Engineers 51:70-75. 1963.

APPENDICES

APPENDIX 1

Derivation of the Huygens-Fresnel Principle

We will derive (1, 4, 34) a certain approximate form of the Huygens-Fresnel principle which can be applied to optical resonator problems.

Maxwell's equations may be written for a linear, isotropic, homogeneous, source-free medium as:

$$\bar{\nabla} \times \bar{E} = -\mu \frac{\partial \bar{H}}{\partial t} \tag{1}$$

$$\bar{\nabla} \times \bar{H} = \epsilon \frac{\partial \bar{E}}{\partial t} \tag{2}$$

$$\mu \bar{\nabla} \cdot \bar{H} = 0 \tag{3}$$

$$\epsilon \bar{\nabla} \cdot \bar{E} = 0 \tag{4}$$

Taking the curl of equations (1) and (2), we have

$$\begin{aligned} \bar{\nabla} \times \bar{\nabla} \times \bar{E} &= -\mu \frac{\partial}{\partial t} (\bar{\nabla} \times \bar{H}) \\ \bar{\nabla} \times \bar{\nabla} \times \bar{H} &= \epsilon \frac{\partial}{\partial t} (\bar{\nabla} \times \bar{E}) \end{aligned} \tag{5}$$

or, after using equations (1) and (2) again,

$$\begin{aligned} \bar{\nabla} \times \bar{\nabla} \times \bar{E} &= -\mu\epsilon \frac{\partial^2 \bar{E}}{\partial t^2} \\ \bar{\nabla} \times \bar{\nabla} \times \bar{H} &= -\mu\epsilon \frac{\partial^2 \bar{H}}{\partial t^2} \end{aligned} \tag{6}$$

Now since $\bar{\nabla} \times \bar{\nabla} \times \bar{A} = \bar{\nabla} (\bar{\nabla} \cdot \bar{A}) - \bar{\nabla}^2 \bar{A}$, and using equations (3) and (4), equations (6) become

$$\bar{\nabla}^2 \bar{E} - \mu\epsilon \frac{\partial^2 \bar{E}}{\partial t^2} = 0$$

$$\bar{\nabla}^2 \bar{H} - \mu\epsilon \frac{\partial^2 \bar{H}}{\partial t^2} = 0 \qquad (7)$$

where $\bar{\nabla}^2$ is the vector Laplacian. Assuming that the fields have an $e^{j\omega t}$ time dependence, equations (7) are

$$\bar{\nabla}^2 \underline{\bar{E}} + k^2 \underline{\bar{E}} = 0 \qquad (8)$$

$$\bar{\nabla}^2 \underline{\bar{H}} + k^2 \underline{\bar{H}} = 0 \qquad (9)$$

where $\bar{E} = \underline{\bar{E}}\, e^{j\omega t}$, $\bar{H} = \underline{\bar{H}}\, e^{j\omega t}$, and $k^2 = \omega^2 \mu\epsilon$ is the propagation constant.

If we choose some rectangular coordinate system x, y, z, then equation (8) can be expanded into

$$\bar{a}_x [\nabla^2 E_x + k^2 E_x] + \bar{a}_y [\nabla^2 E_y + k^2 E_y] + \bar{a}_z [\nabla^2 E_z + k^2 E_z] = 0 \qquad (10)$$

where $\bar{a}_x$, $\bar{a}_y$, and $\bar{a}_z$ are unit vectors in the x, y, and z directions, and $\underline{\bar{E}} = \bar{a}_x E_x + \bar{a}_y E_y + \bar{a}_z E_z$, where E_x, E_y, and E_z are scalars. A similar expansion can be written for equation (9). We conclude that E_x, E_y, E_z, H_x, H_y, and H_z each satisfy the scalar Helmholtz equation:

$$\nabla^2 u + k^2 u = 0 \qquad (11)$$

where

$$u = E_x; E_y; \ldots . H_z.$$

Now let V be a source free volume bounded by a closed surface s, and let P be any point within V (see Figure 14). Assume that the

scalar u(x, y, z), which represents any one of the rectangular components of the field vectors, has continuous first and second partial derivatives within V and on s. Let v be any other function which satisfies the same continuity requirements as u. Then by a scalar Green's theorem,

$$\int_V (u\nabla^2 v - v\nabla^2 u)\, dv = -\int_s (u \frac{\partial v}{\partial n} - v \frac{\partial u}{\partial n})\, ds \qquad (12)$$

where $\frac{\partial}{\partial n}$ denotes differentiation along an inward normal of s. We have shown that u satisfies the scalar Helmholtz equation; if v does also, then the integrand of the volume integral in equation (12) vanishes, and we have:

$$\int_s (u \frac{\partial v}{\partial n} - v \frac{\partial u}{\partial n})\, ds = 0 \qquad (13)$$

Now let

$$v = \frac{e^{-ikr}}{r} \qquad (14)$$

where r is the distance from p to any other point in v, and k is the propagation constant. Equation (14) describes the isotropic radiation field of a point source stationed at r = 0. This function v has a singular point at p, and since we assumed that v was continuous and differentiable within v, point p must be excluded from the region of integration in equations (12) and (13).

Surround point p with a sphere of radius ϵ which has a surface s'. Now volume V is bounded by surfaces s and s'. Equation (13)

must be replaced by

$$\int_s (u \frac{\partial v}{\partial n} - v \frac{\partial u}{\partial n}) \, ds + \int_{s'} (u \frac{\partial v}{\partial n} - v \frac{\partial u}{\partial n}) \, ds = 0 \qquad (15)$$

Now

$$\frac{\partial v}{\partial n} = \bar{n} \cdot \bar{\nabla} v = \bar{n} \cdot \bar{a}r \frac{\partial v}{\partial r}$$

or

$$\frac{\partial v}{\partial n} = - \frac{e^{-ikr}}{r} (ik + 1/r) \cos (\bar{n}, \bar{r}) \qquad (16)$$

where $\bar{a}r$ is a unit rector in the direction of increasing r and $(\bar{n}, \bar{r})$ denotes the angle between a normal into the volume V and the vector $\bar{r}$ (see Figure 14). On the surface s', $\cos (\bar{n}, \bar{r}) = 1$, and equation (15) may be written as

$$\int_s (u \frac{\partial v}{\partial n} - v \frac{\partial u}{\partial n}) \, ds = - \int_{s'} (- \frac{e^{-ikr}}{r} (ik + 1/r) u - \frac{e^{-ikr}}{r} \frac{\partial u}{\partial n}) \, ds \qquad (17)$$

On the surface s', $r = \epsilon$, and $ds = \epsilon^2 d\Lambda$, where $d\Lambda$ is an element of solid angle. Then equation (17) becomes

$$\int_s (u \frac{\partial v}{\partial n} - v \frac{\partial u}{\partial n}) \, ds = \int_\Lambda e^{-ik\epsilon} (iku\epsilon + u + \epsilon \frac{\partial u}{\partial n}) \, d\Lambda \qquad (18)$$

Now take the limit of equation (18) as $\epsilon \to 0$. This gives

$$\int_s (u \frac{\partial v}{\partial n} - v \frac{\partial u}{\partial n}) \, ds = u_p \int_\Lambda d\Lambda$$

or,

$$u_p = \frac{-1}{4\pi} \int_s \left(u \frac{\partial v}{\partial n} - v \frac{\partial u}{\partial n}\right) ds \qquad (19)$$

where u_p means the value of u (x, y, z) at the coordinates of point p. Using equation (16), equation (19) can be written as

$$u_p = \frac{1}{4\pi} \int_s \frac{e^{-ikr}}{r} \left[(ik + 1/r)\, u \cos(\overline{n}, \overline{r}) + \frac{\partial u}{\partial n} \right] ds \qquad (20)$$

Equation (20) is a scalar form of the Huygens-Fresnel principle. It gives the field at a point p in the volume v in terms of the field on the boundary of v, the surface s. Note that the field at p is composed of contributions from all points of the surface s.

We have said that there are no sources inside closed surface s, therefore any sources must be located outside s. Consider the region far from the sources. We want an approximation to equation (20) for surfaces s in this region. Choose an origin near the point p, and let ρ, θ, ϕ be the spherical coordinates of a point in the far zone with respect to this origin (see Figure 14). Assume that in the far zone the field caused by the sources has an amplitude function which can be written (34) as:

$$u = \frac{e^{ik\rho}}{\rho} F(\theta, \phi) \qquad (21)$$

Equation (21) describes waves propagating toward $\rho = 0$ which have spherical phase fronts centered on $\rho = 0$. This is a simplifying assumption which will enable us to apply equation (20) to optical resonator problems. If $\overline{n}$ is a normal inward from s and $\overline{\rho}_1$, $\overline{\theta}_1$, $\overline{\phi}_1$

are unit vectors in the direction of increasing ρ, θ, ϕ at a point on s, then at the point on s

$$\frac{\partial u}{\partial n} = \bar{n} \cdot \bar{\nabla} u = \bar{n} \cdot \left(\frac{\partial u}{\partial \rho} \bar{\rho}_1 + \frac{1}{\rho} \frac{\partial u}{\partial \theta} \bar{\theta}_1 + \frac{1}{\rho \sin\theta} \frac{\partial u}{\partial \phi} \bar{\phi}_1\right) \qquad (22)$$

Using equation (21) we can write

$$\bar{\nabla} u = iku \bar{\rho}_1 + \frac{u}{\rho} \left(\bar{\rho}_1 + \frac{1}{F} \frac{\partial F}{\partial \theta} \bar{\theta}_1 + \frac{1}{F \sin\theta} \frac{\partial F}{\partial \phi} \bar{\phi}_1\right) \qquad (23)$$

Consider only points p such that $\rho \gg \lambda$ (and thus $r \gg \lambda$) for all points on s. Then $k \gg 1/\rho$, and if the variation of u in the θ and ϕ directions is small compared to that in the radial direction, then

$$\bar{\nabla} u \cong iku \bar{\rho}_1$$

and

$$\frac{\partial u}{\partial n} = \bar{n} \cdot \bar{\nabla} u \cong iku \cos(\bar{n}, \bar{\rho}_1) \qquad (24)$$

Now equation (20) becomes

$$u_p \cong \frac{-1}{4\pi} \int_s \frac{e^{-ikr}}{r} \left\{iku\left[\cos(\bar{n}, \bar{r}) + \cos(n, \rho_1)\right] + \frac{u}{r} \cos(\bar{n}, \bar{r})\right\} ds \qquad (25)$$

But since $k \gg 1/r$ for all points on s, the u/r term is negligible compared to the iku term, and equation (25) may be written

$$u_p \cong \frac{-ik}{2\pi} \int_s u \cos(\bar{n}, \bar{r}) \frac{e^{-ikr}}{r} ds \qquad (26)$$

noting that $\cos(\bar{n}, \bar{\rho}_1) \cong \cos(\bar{n}, \bar{r})$. Equation (26) is the approximate form of the Huygens-Fresnel principle which we desire.

To reiterate, if a point p is in a linear, isotropic, homogeneous source-free medium and is enclosed by a closed surface s, and if point p and surface s are located in the far zone of the sources, and if point p is such that $r \gg \lambda$ for all points on s, then the field at p is given in terms of the field on s by equation (26), if the field on s can be described by equation (21).

APPENDIX 2

Phase Shift Across Confocal Mirrors

We have said that the mirrors of a confocal resonator are constant phase surfaces. Actually there is a small phase shift across the mirrors. Consider Figure 16. The mirror M_2 crosses the z axis at z_o, and in the xz plane M_2 defines a segment of the circle

$$(z + b - z_o)^2 + x^2 = b^2 \tag{1}$$

Define $\Delta z = z_o - z$. Then

$$(b - \Delta z)^2 + x^2 = b^2 \tag{2}$$

Solving for Δz, we find

$$\Delta z = b \pm b\sqrt{1 - x^2/b^2}$$

Taking the minus sign, since Δz increases with increasing x, and using the binomial expansion, we find

$$\Delta z \cong \frac{x^2}{2b} + \frac{x^4}{8b^3} \tag{3}$$

for $x \ll b$.

The constant phase surfaces of the confocal resonator are given by

$$\Delta z' = \frac{\zeta_o}{1 + \zeta_o^2} \frac{w^2}{b}$$

where $\Delta z' = z_o - z$, $\zeta_o = \frac{2z_o}{b}$, and $w^2 = x^2 + y^2$. The constant phase

surface interesecting the z axis at $z_o = b/2$ defines a line in the xz plane

$$\Delta z' = \frac{x^2}{2b} \qquad (4)$$

Then the phase over the mirror leads the phase over the constant phase surface by an amount $\Delta\phi$, where

$$\Delta\phi \cong k(\Delta z - \Delta z') = \frac{kx^4}{8b^3} \text{ radians}$$

and $k = 2\pi/\lambda$. For a typical case, $b = 100$ cm and $\lambda = 10^{-4}$ cm. At the edge of the dominant mode spot ($x = .06$ cm) we find

$$\Delta\phi \cong 10^{-7} \text{ radian}$$

Because this phase shift is so small, the confocal mirrors are essentially constant phase surfaces.

APPENDIX 3

Figures

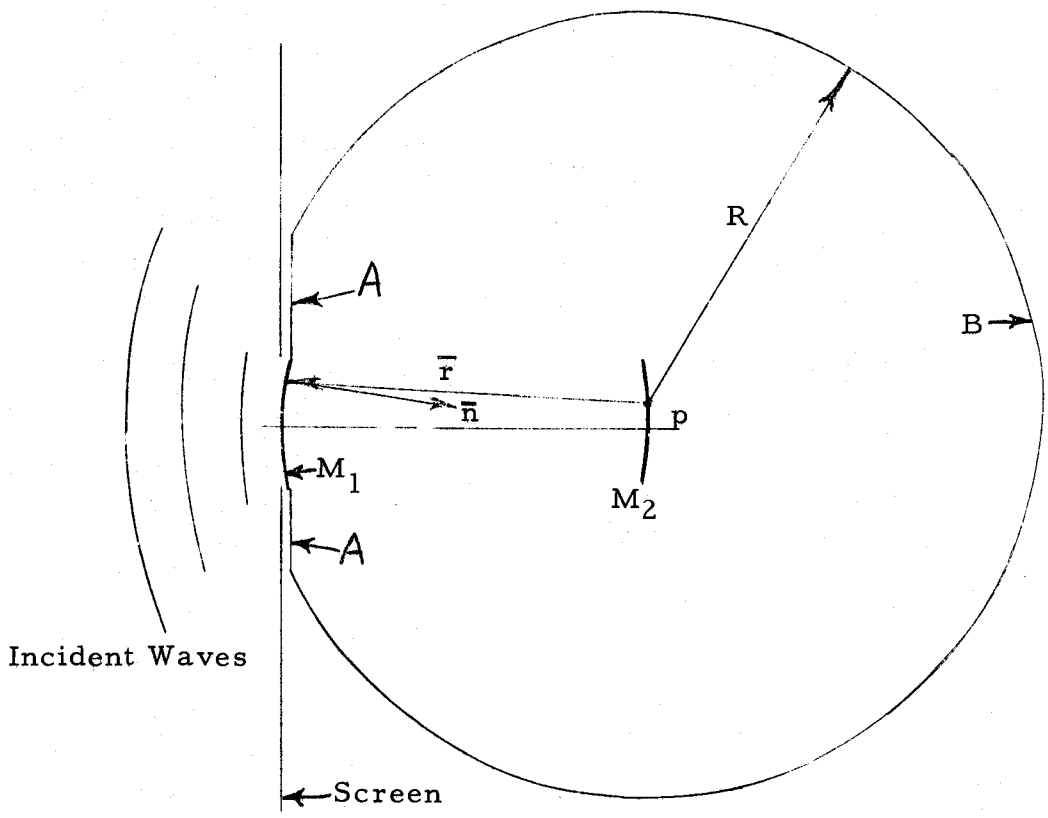

Figure 1. An illustration of the application of the Huygens-Fresnel principle to resonator problems. M_1 and M_2 represent mirrors of a spherical mirror resonator. This principle gives the field at point p in terms of the field on surfaces M_1, A and B which enclose p (4).

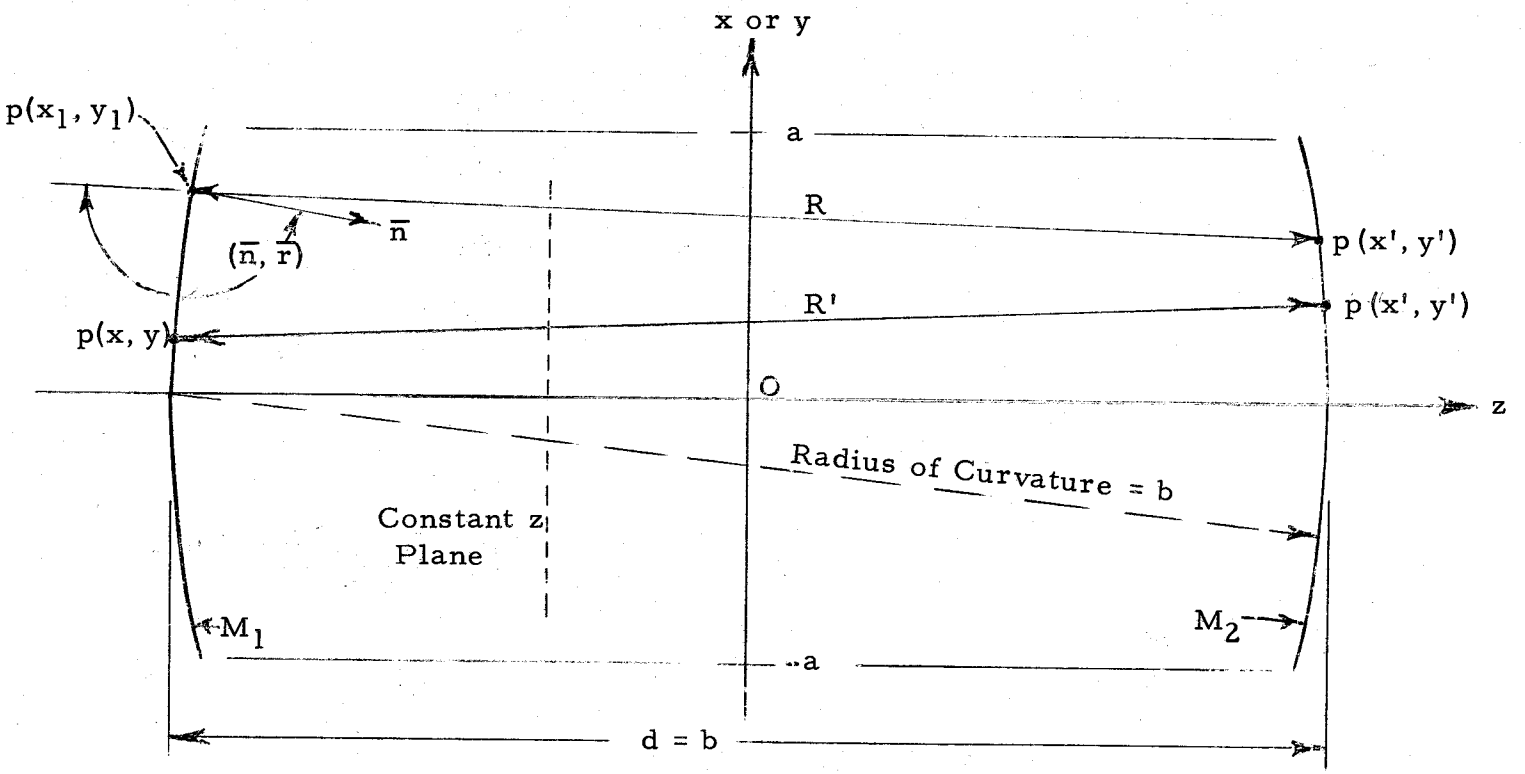

Figure 2. Representation of a spherical mirror resonator with confocal spacing. M_1 and M_2 are spherical mirrors. Redrawn from (5).

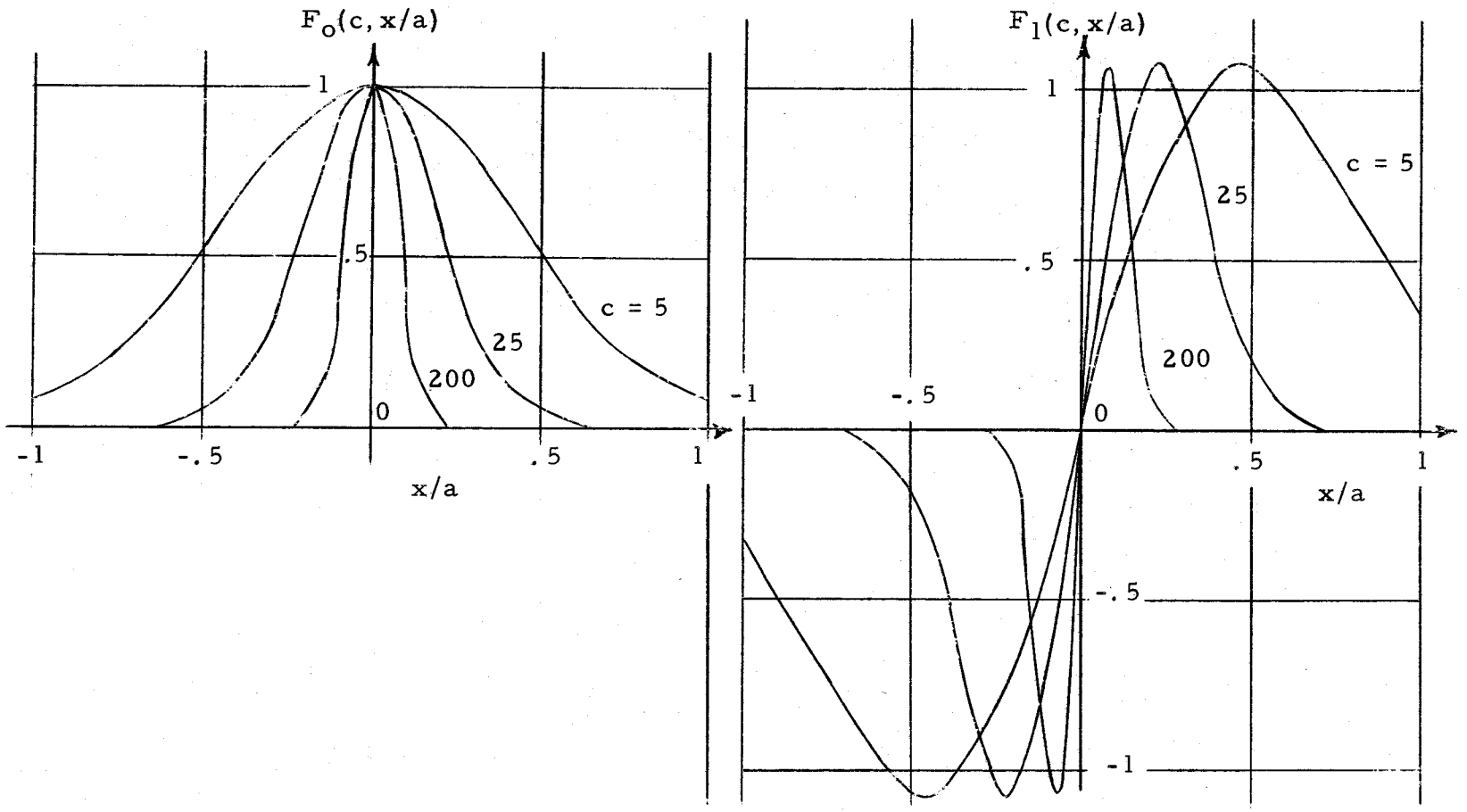

Figure 3. Approximate field amplitude variation across the mirrors of a confocal resonator. F_o and F_1 are eigenfunctions given by equation (2-19) with m = 0 and 1. The normalized distance from the mirror center is x/a, where a is the mirror half width. The parameter $c = 2\pi(a^2/b\lambda)$. Redrawn from (5).

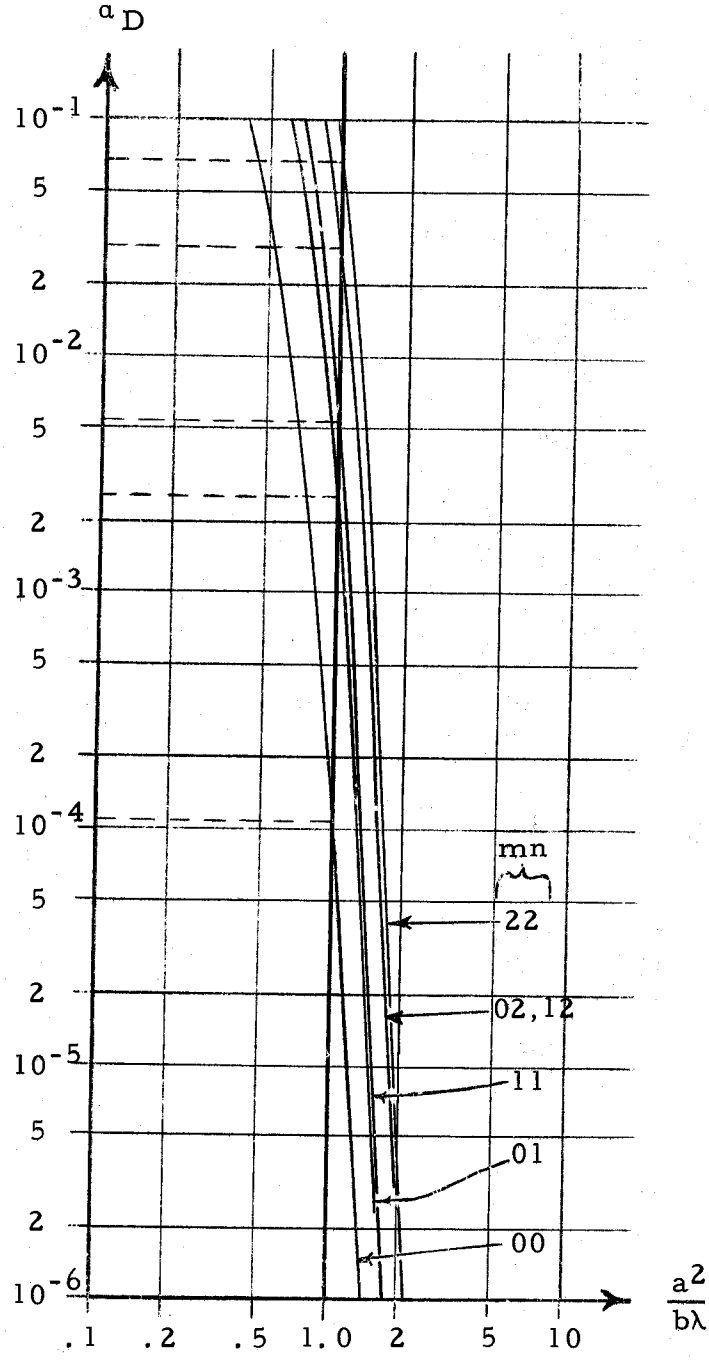

Figure 4. Diffraction losses of the confocal resonator. The fractional diffraction loss α_D is shown as a function of the Fresnel number $a^2/b\lambda$ for the five modes of lowest transverse order. Redrawn from (5).

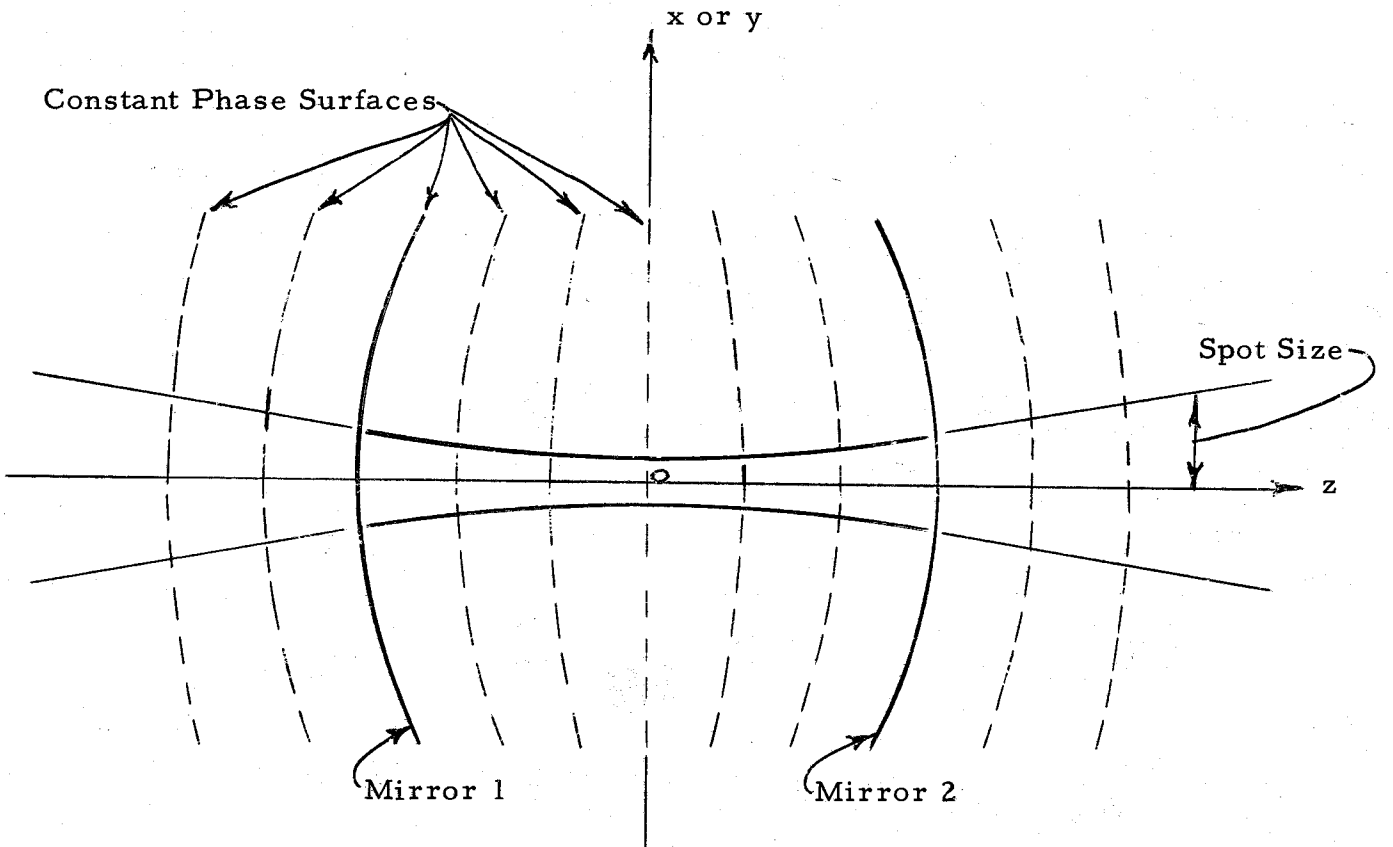

Figure 5. Constant phase surfaces and spot size of a confocal resonator. The dashed lines represent constant phase surfaces generated by the confocal resonator, and the hyperbolic curves indicate the variation of spot size with z.

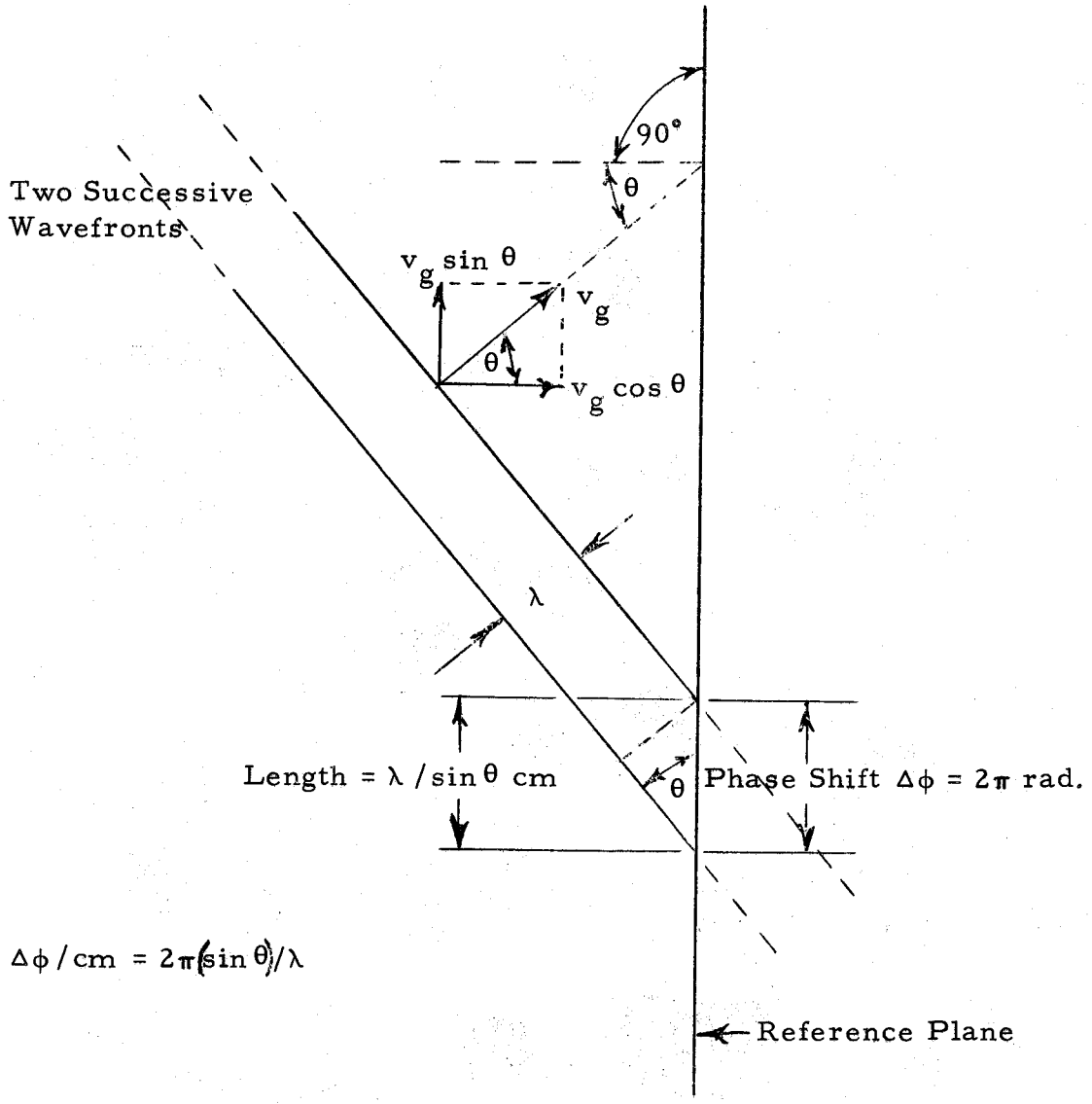

Figure 6. Resolution of a plane wave passing a reference plane into components normal to and parallel to the reference plane. The wave is incident on the reference plane at an angle θ and with group velocity v_g. The normal component of the wave has group velocity $v_g \cos \theta$, and the parallel component has group velocity $v_g \sin \theta$.

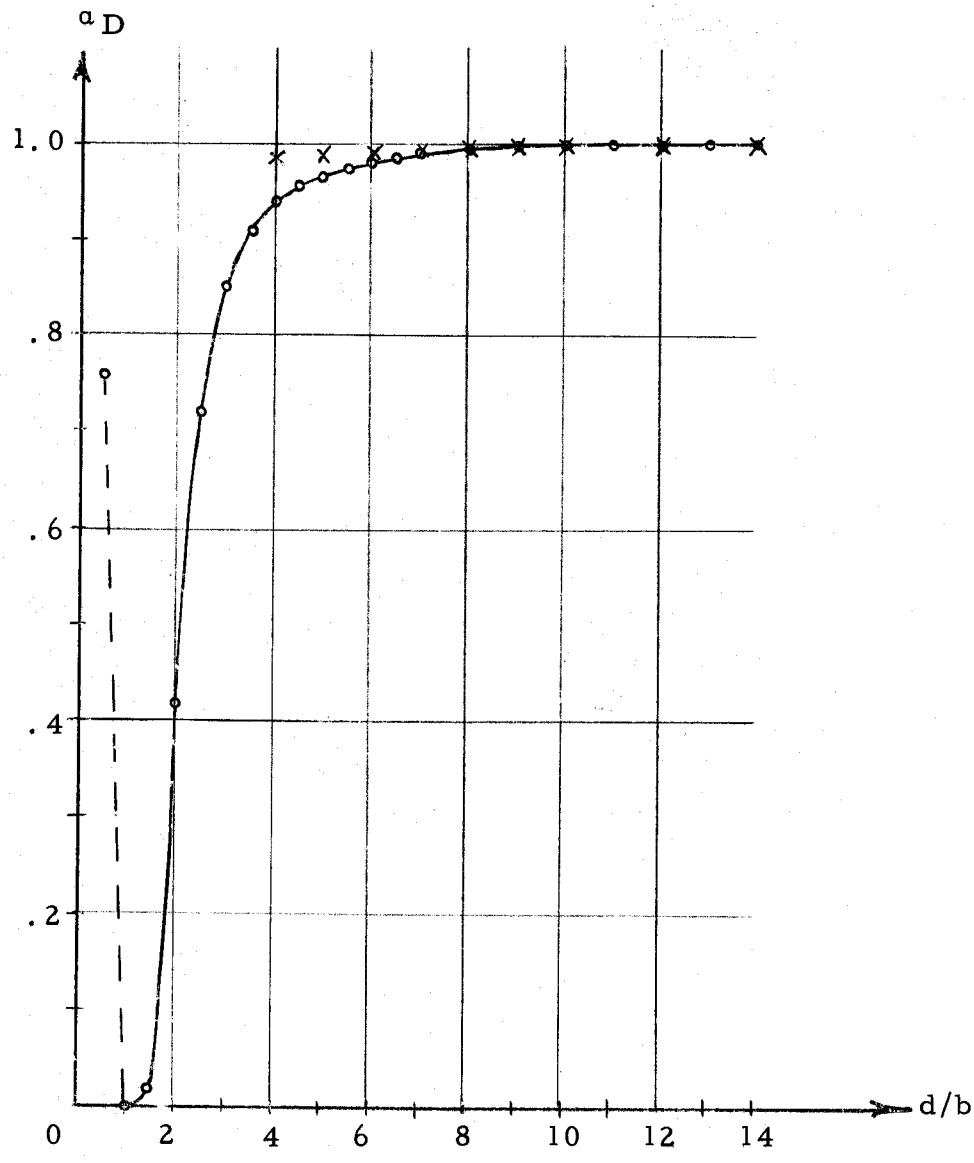

Figure 7. Fractional diffraction loss α_D as a function of d/b for a nonconfocal resonator. The resonator has identical mirrors with radii of curvature b spaced a distance d apart. The crosses are predictions of equation (3-21): $\alpha_D = 1 - (b/2d)^2$. Redrawn from (36).

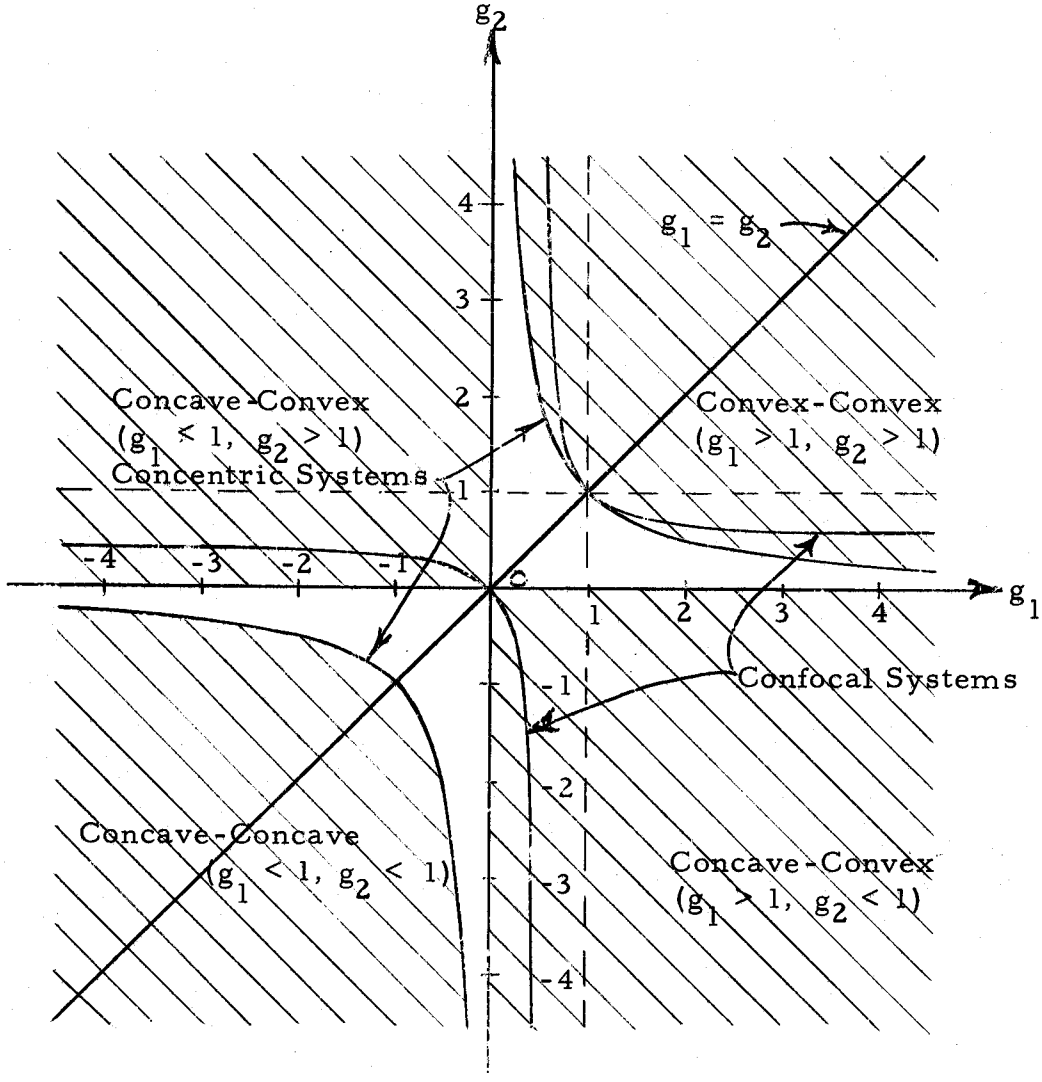

Figure 8. Resonator loss diagram. The resonator has mirrors with radii of curvature b_1 and b_2 spaced a distance d apart. This diagram is a representation of the stability condition, $0 \leq g_1 g_2 \leq 1$, where $g_1 = 1 - d/b_1$ and $g_2 = 1 - d/b_2$. A given resonator is represented by a single point on the diagram. Resonators lying in the crosshatched regions are unstable (high loss), while resonators lying in the other regions are stable (low loss). Resonators with mirrors having equal radii of curvature lie on the line $g_1 = g_2$. Redrawn from (11).

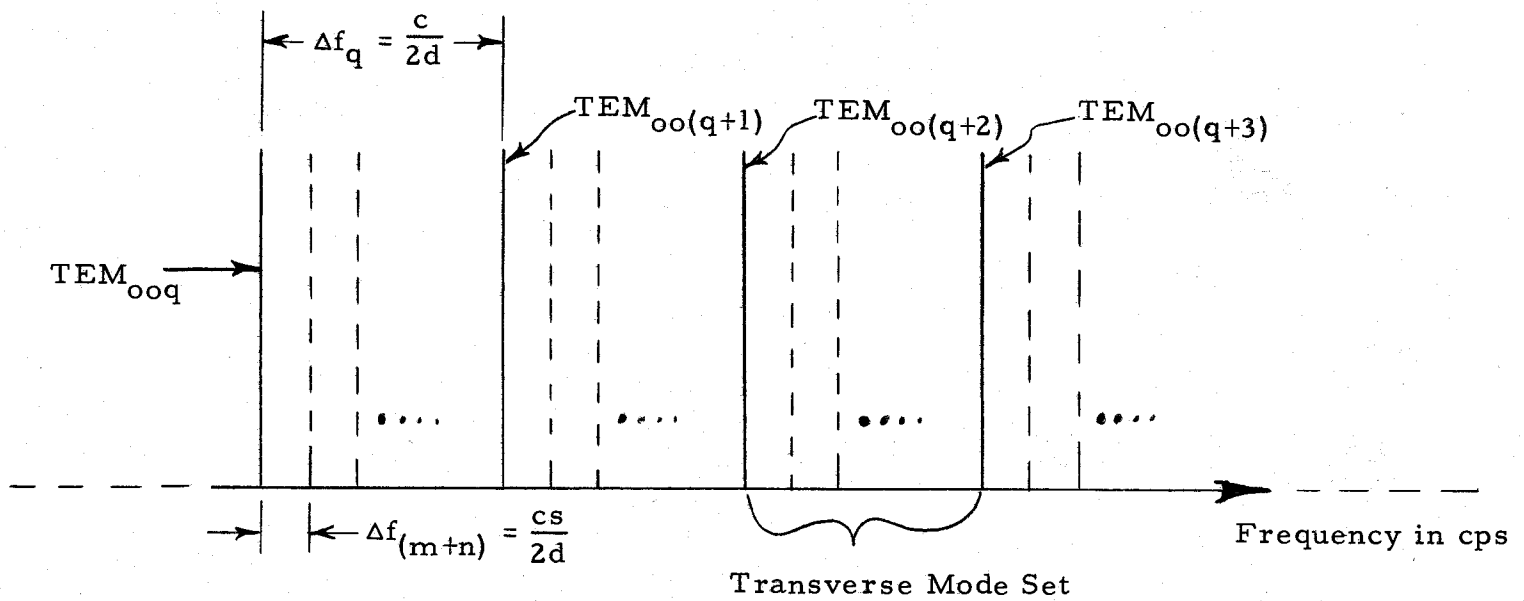

Figure 9. Representation of a section of the frequency spectrum of a spherical mirror resonator. The solid vertical lines represent dominant mode resonances, and the dashed lines represent higher transverse order resonances. The quantities Δf_q and $\Delta f_{(m+n)}$ are the frequency separations between adjacent longitudinal and transverse resonances, respectively.

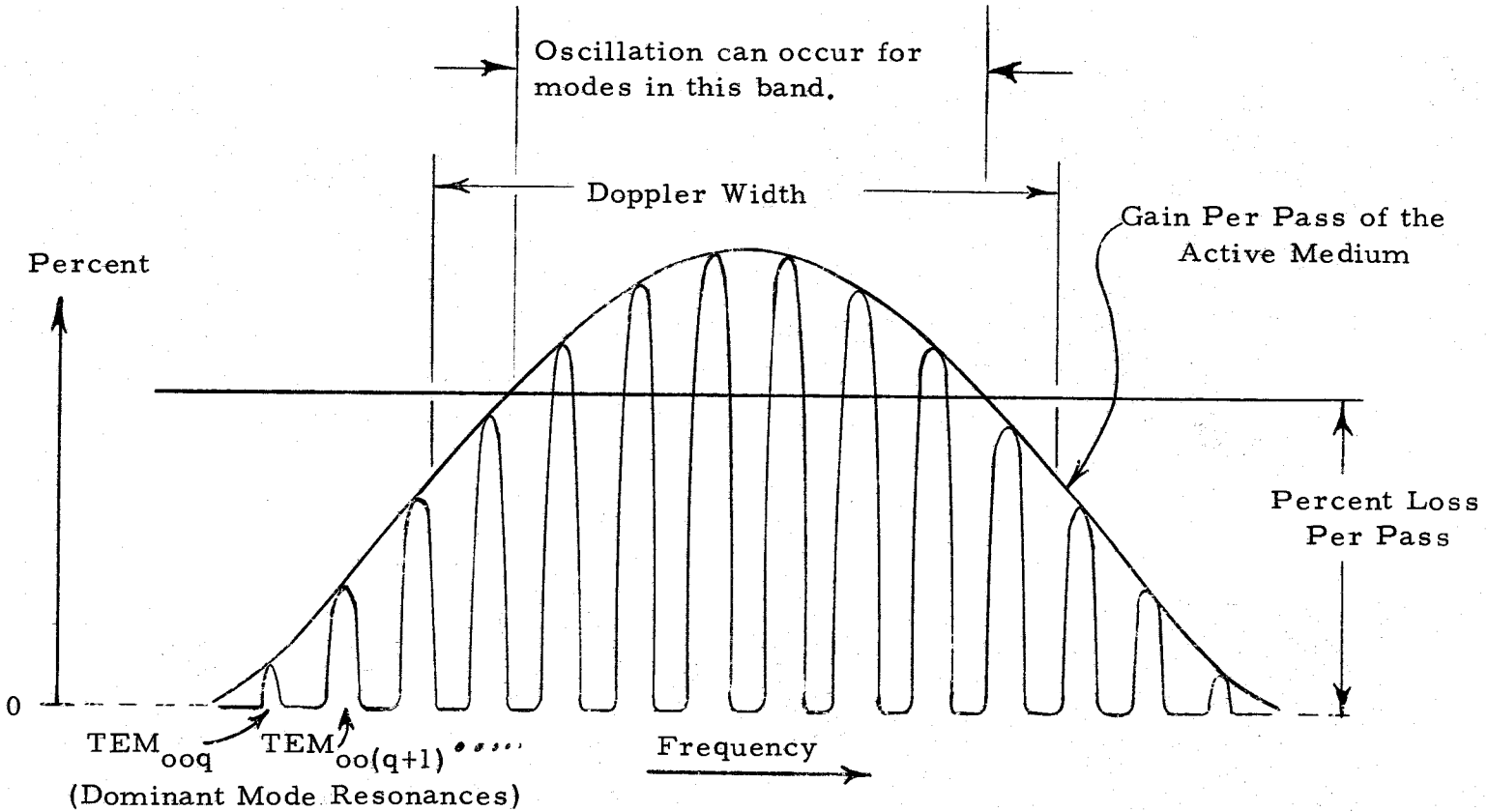

Figure 10. Interaction of normal mode resonances and a laser active medium. Oscillation can occur in those modes for which the gain per pass exceeds the loss per pass. Redrawn from (24).

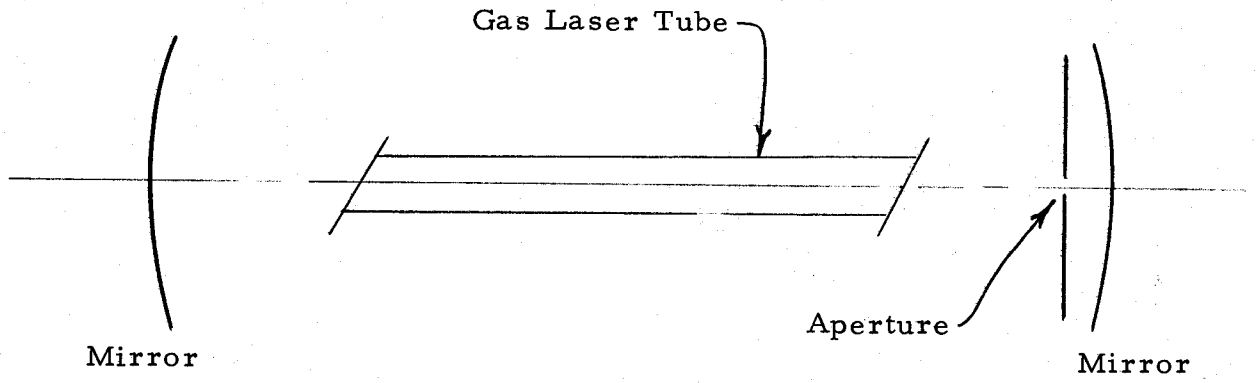

Figure 11. Laser with aperture mode selector. The aperture selects the dominant transverse mode.

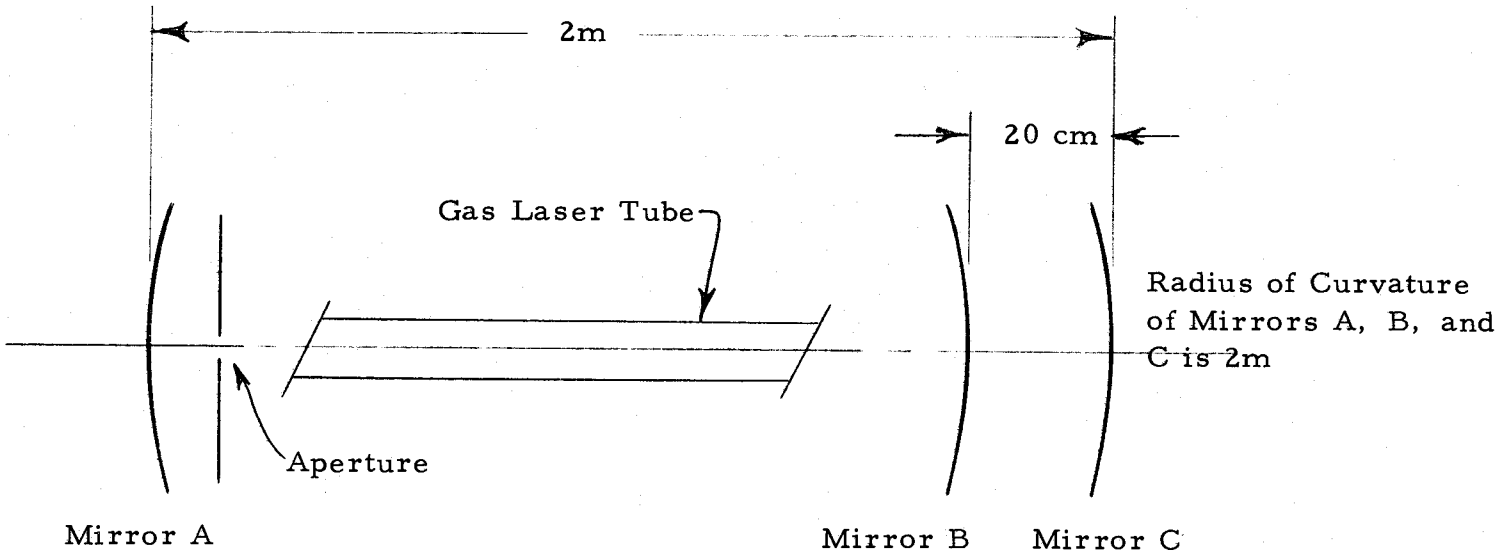

Figure 12. Laser with single frequency output. The aperture selects the dominant transverse mode, and proper positioning of mirror C eliminates all but one longitudinal mode through interference effects. Redrawn from (21).

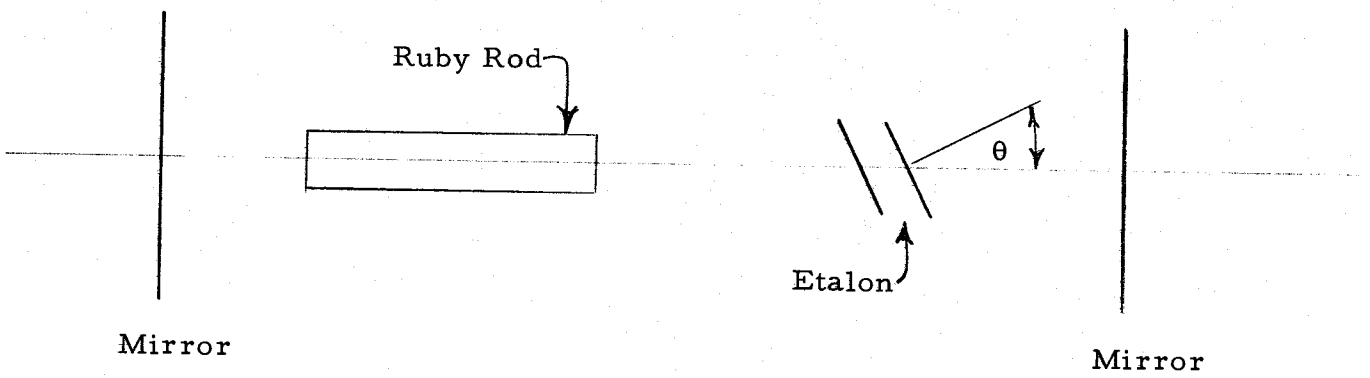

Figure 13. Laser with Fabry-Perot etalon mode selector. Interference effects in the etalon discriminate among longitudinal modes, and the angular passband characteristics of the etalon favor lower order transverse modes. Redrawn from (8).

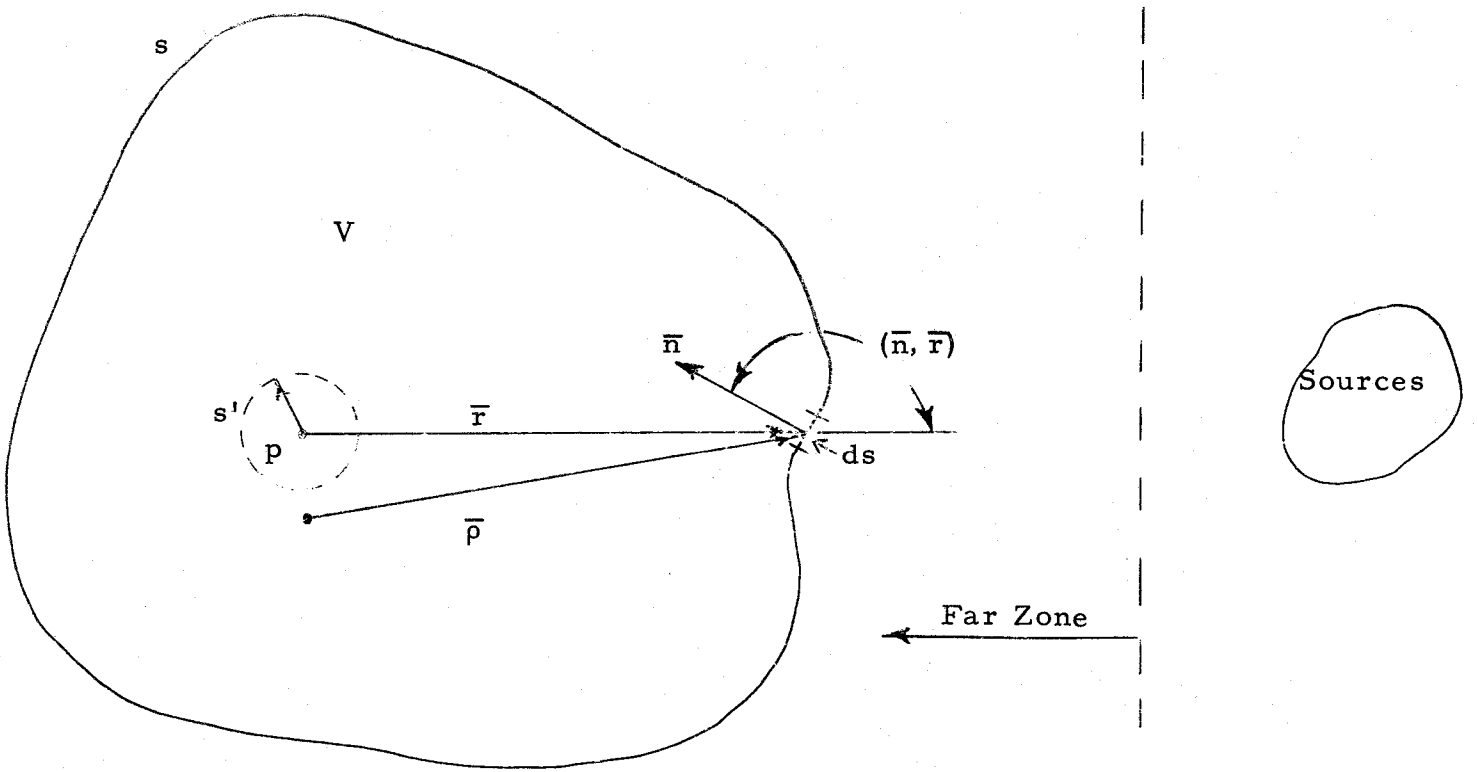

Figure 14. Illustration used in deriving the Huygens-Fresnel principle. (See Appendix 1).

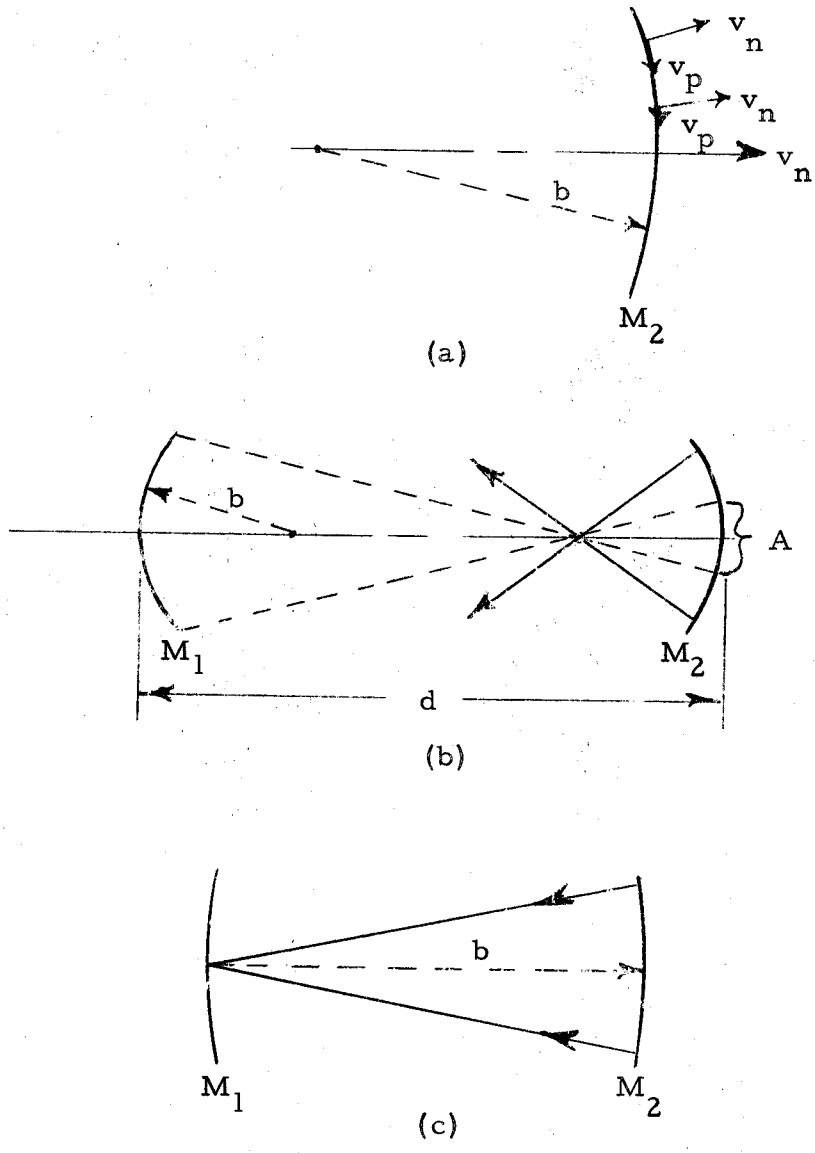

Figure 15. (a) Resolution of the incident wave (for the d ≫ b case) into components normal to and parallel to the mirror.

(b) Loss predicted by geometrical optics for the d ≫ b case. Waves incident outside A miss the other mirror.

(c) The focussing action of the confocal resonator.

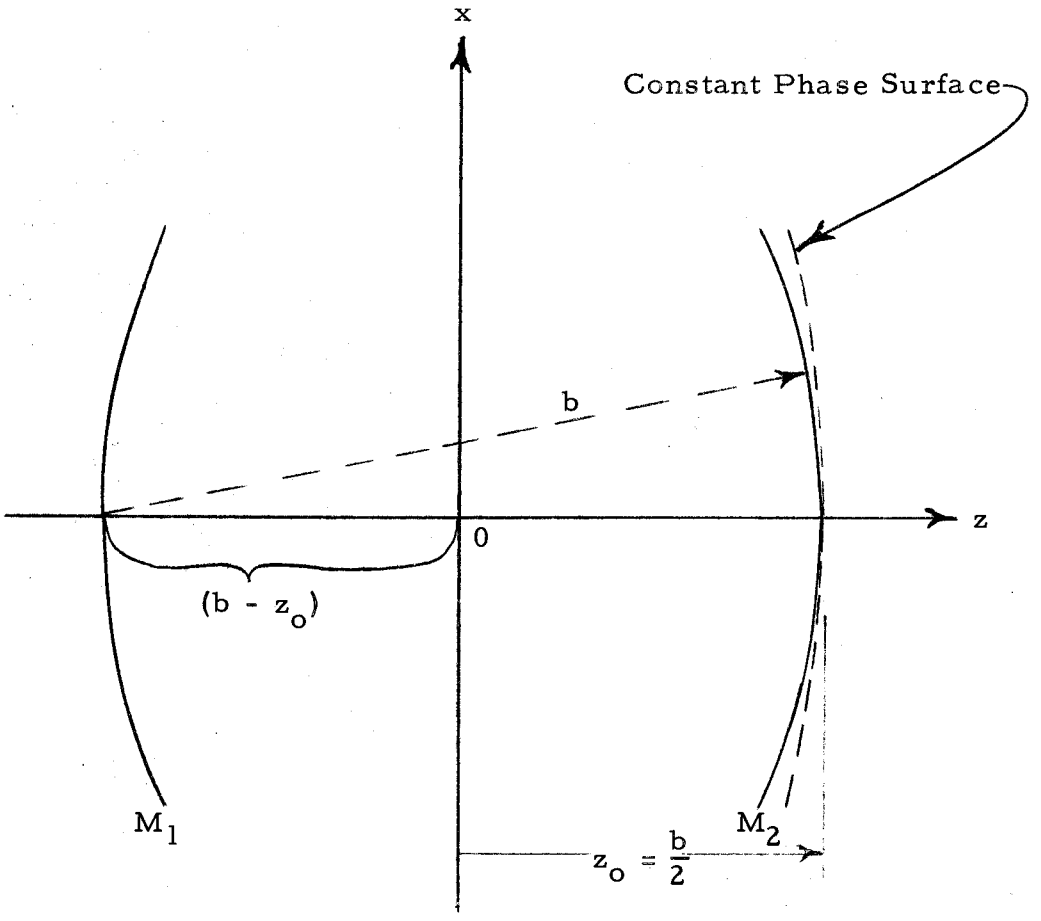

Figure 16. Deviation of a confocal resonator mirror from a constant phase surface. (See Appendix 2).